Low-Temp. Atmospheric Plasma Simulations for Biomedical Appls.

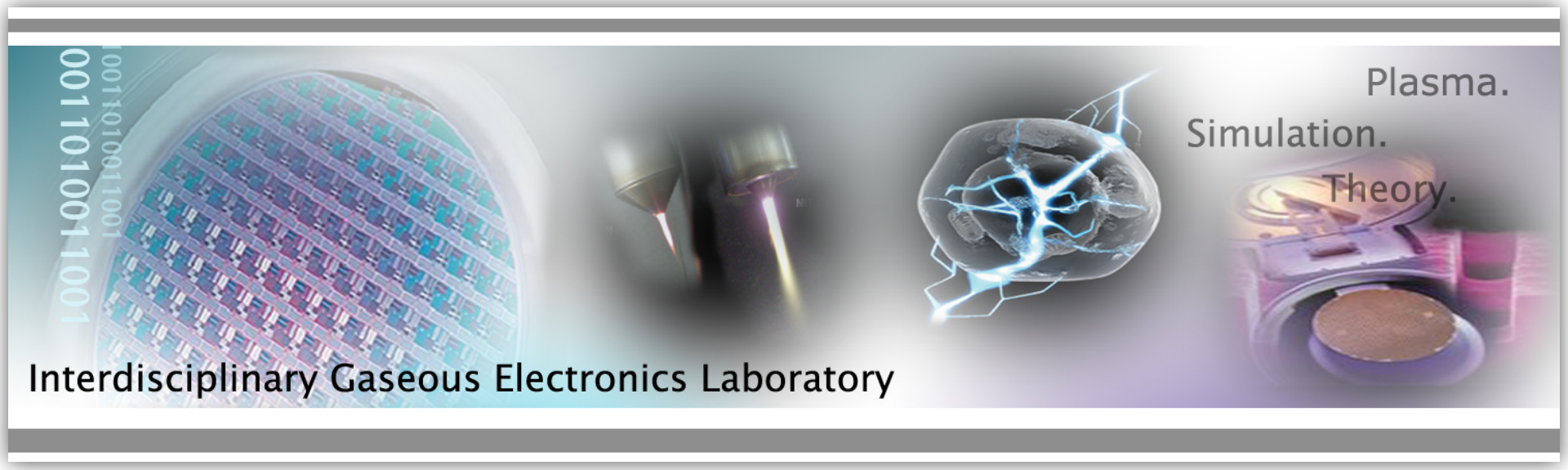

J.K. Lee, S.K. Kang, H.W. Lee, H.C. Kwon, M.S. Kim, H. Y. Kim, H. K. Shin

Department of Electrical Engineering

POSTECH

Introduction

- The physical parameter (plasma particles per Debye region): N_D
- ✓ PIC: numerical parameters
  a. *Cell size* Δx
  b. Time step Δt
  c. *The number of superparticles* per cell, N_c

- limited by

  a. Δx should be **smaller than** (Debye length, sheath length and Larmor radius)
  b. Δt should be **smaller than** (Inverse of plasma frequency, RF driving frequency and maximum collision frequency)
  c. N_c for atmospheric plasma PIC ?
  d. Physical and Numerical Uses of $\mathbf{N_D}$ (Debye Number) in PIC

Scientific Progress (F Iza)

Exponential growth of plasma-enabled technologies

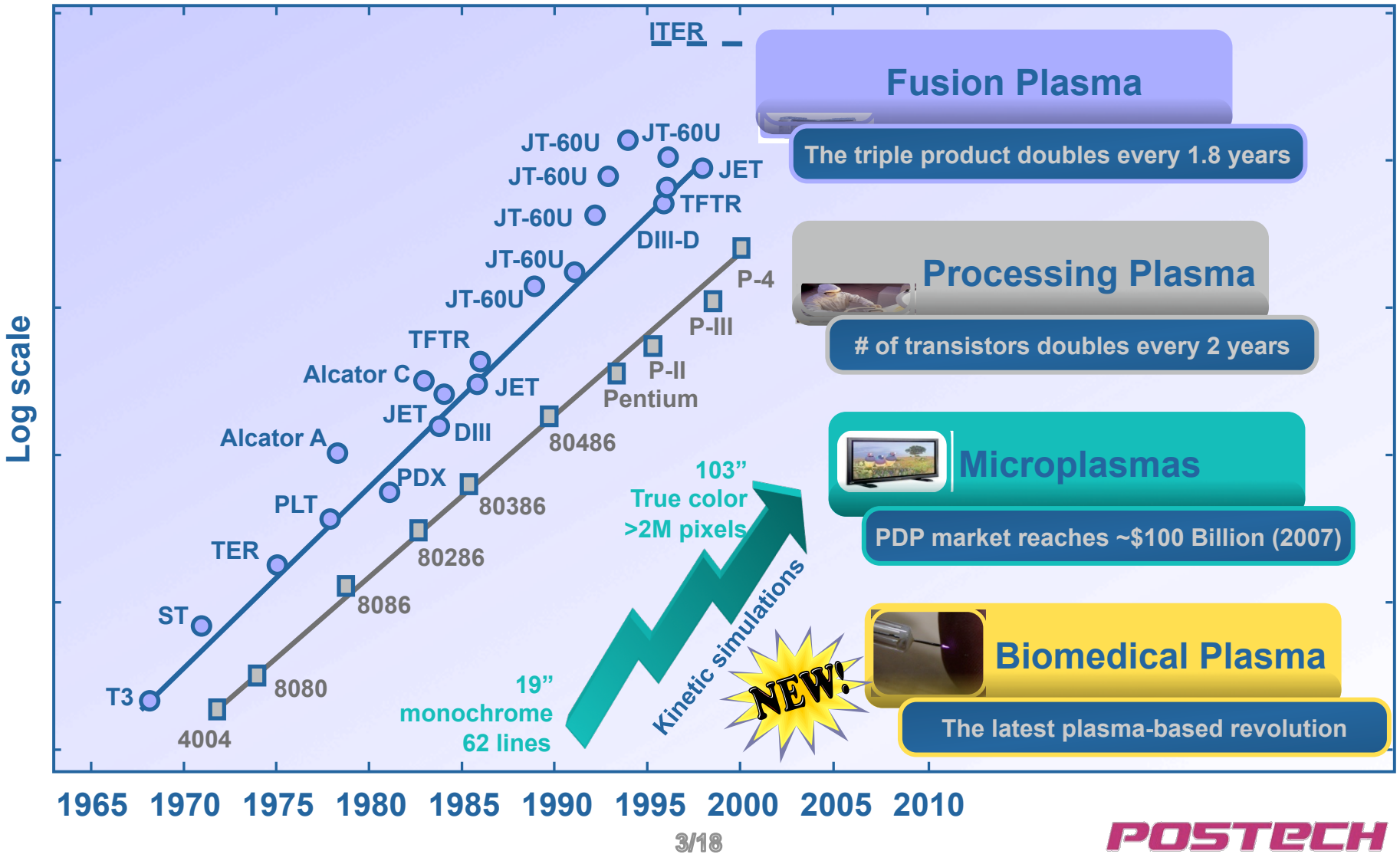

POSTECH

Simulation results give quantitative agreement with measurements.

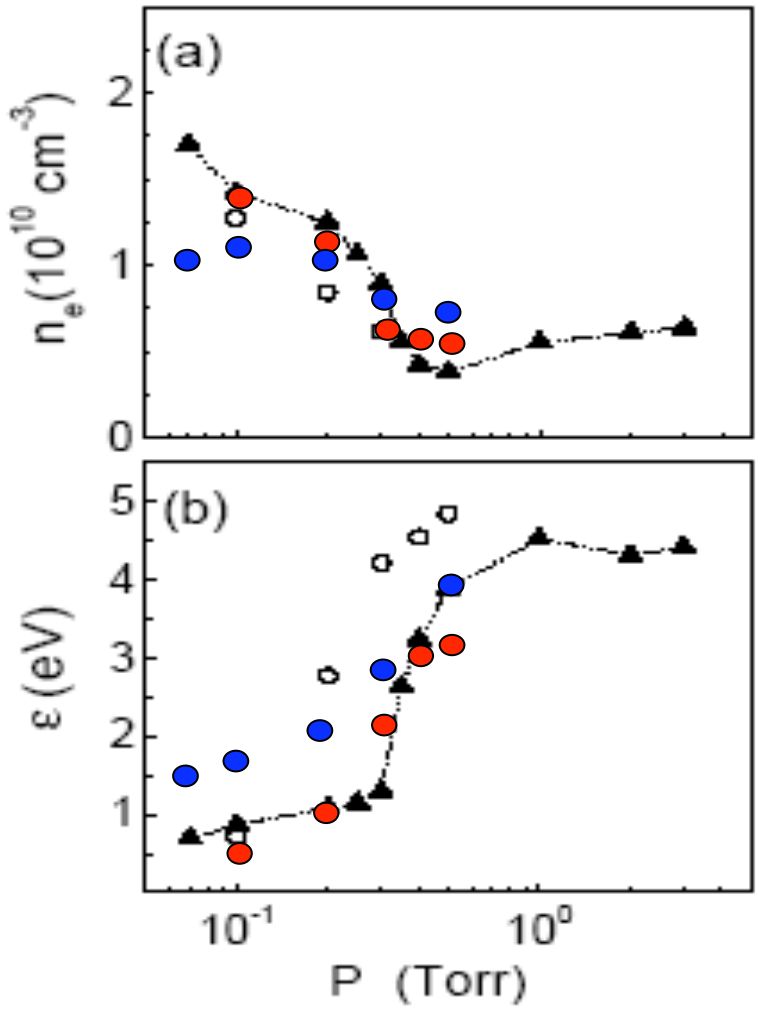

- ● PIC-MCC, H.C.Kim et al, N ~ 1.2e5
- ○ New combined PIC-MCC N ~ 5000
  I.V. Schweigert et al, PSST (2004)
- ● PIC-MCC, Vahedi et al, PSST (1994)
- ▲ Experiment, Godyak et al.(1992)
  Lieberman & Lichtenberg:
  Fig. 11-13 (1st ed.)

✓ argon gas

✓ current density : $2.65 mA/cm^2$

✓ gap distance : 2 cm

[Ref.] H.C. Kim, O. Manuilenko and J.K. Lee, Jpn. J. Appl. Phys. 44, 1957 (2005)

The main reason for better simul. agreement=superparticle number

EEDF for CCP: PIC agrees with probe, not with LTS.

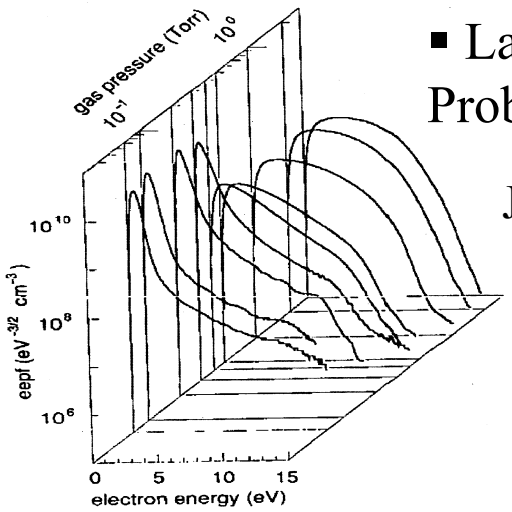

- Langmuir Probe by Godyak

J = 2.65

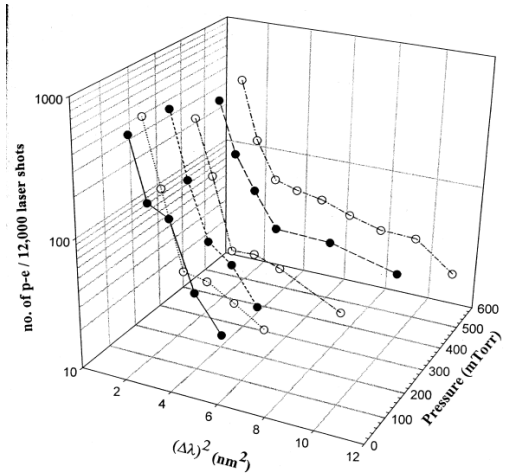

- Laser Thomson Scattering by Elsabbagh

J = 3.8 mA/cm2

Ar, J = 0.38 mA/cm^2

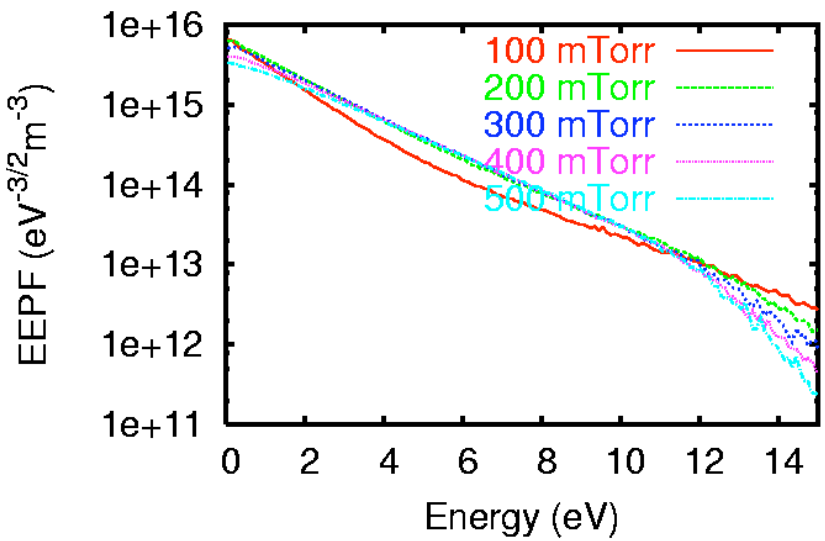

- Using PIC-MCC Simulation

J = 3.8 mA/cm2

[Ref.] H.C. Kim, F. Iza, S.S. Yang, M. Radmilovic-Radjenovic, and J.K. Lee, J. Phys. D: Appl. Phys. 38 R283-R301 (2005)

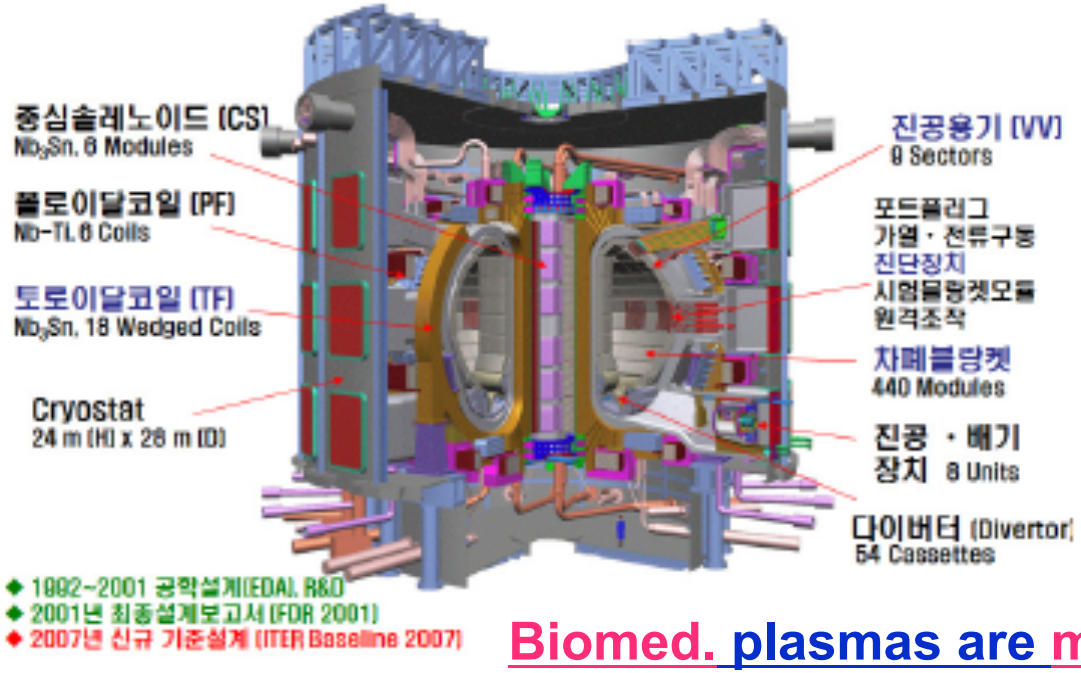

◆ 1992~2001 공학설계(EDA), R&D
◆ 2001년 최종설계보고서 (FDR 2001)
◆ 2007년 신규 기준설계 (ITER Baseline 2007)

그림 1. ITER 설계 모형.

Biomed. plasmas are microplasmas at atmospheric pressure

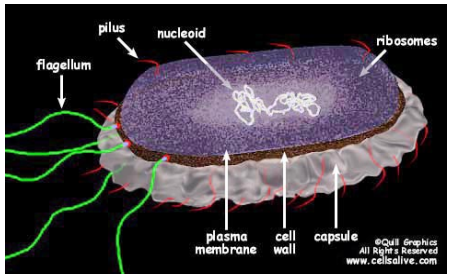

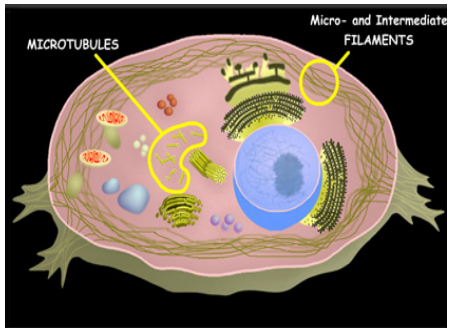

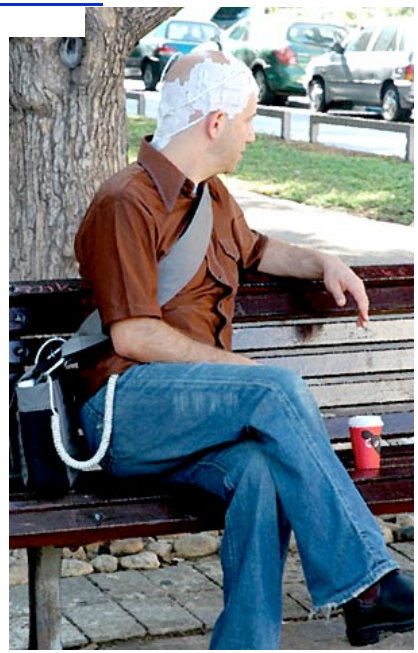

iGEL PLASMA

Electron Kinetics in RF Atmospheric-Pressure Microplasmas

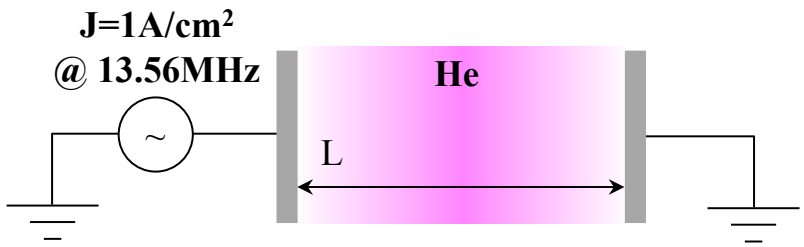

pd ~ 15-6 Torr-cm

Evolution of the electron density profile

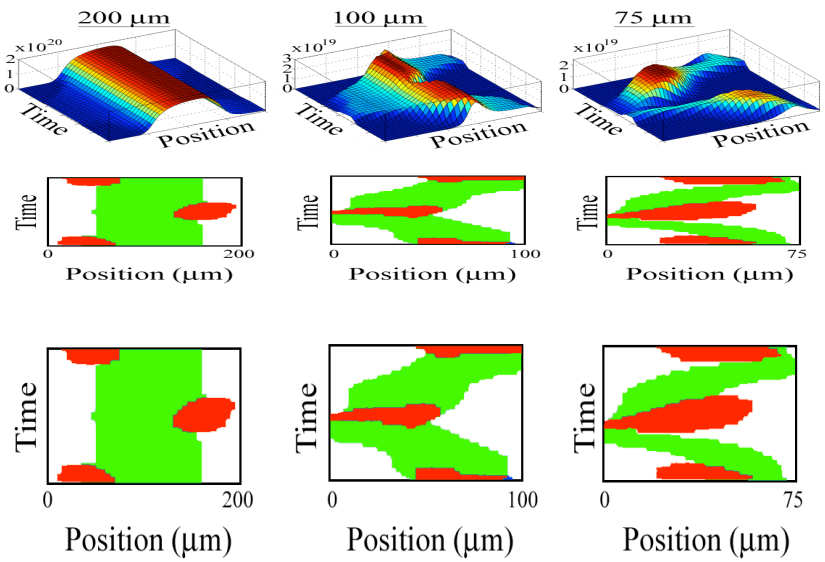

Evolution of EEPF

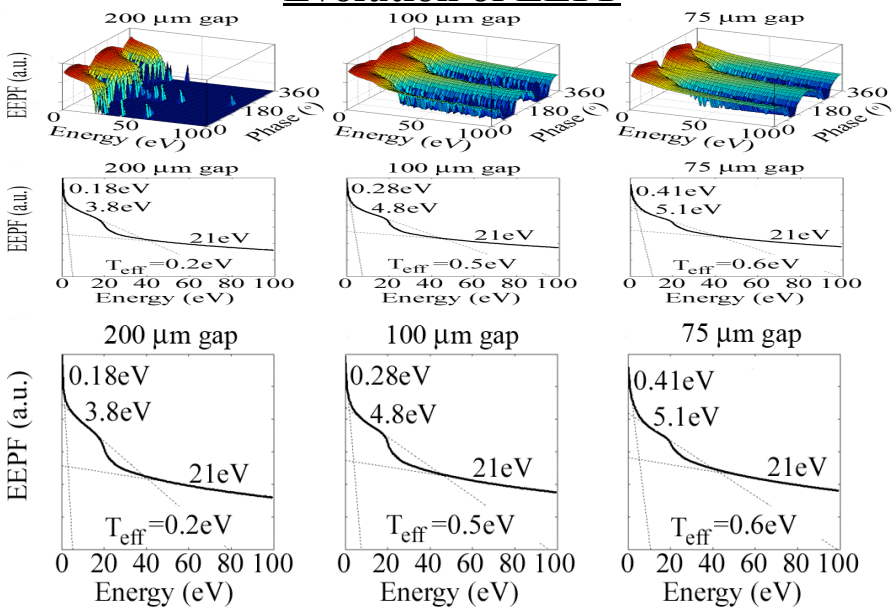

[Ref.] F. Iza, J. K. Lee, and M. G. Kong, Phys. Rev. Lett. 99, 075004 (2007)

Global model / Fluid / PIC-MCC

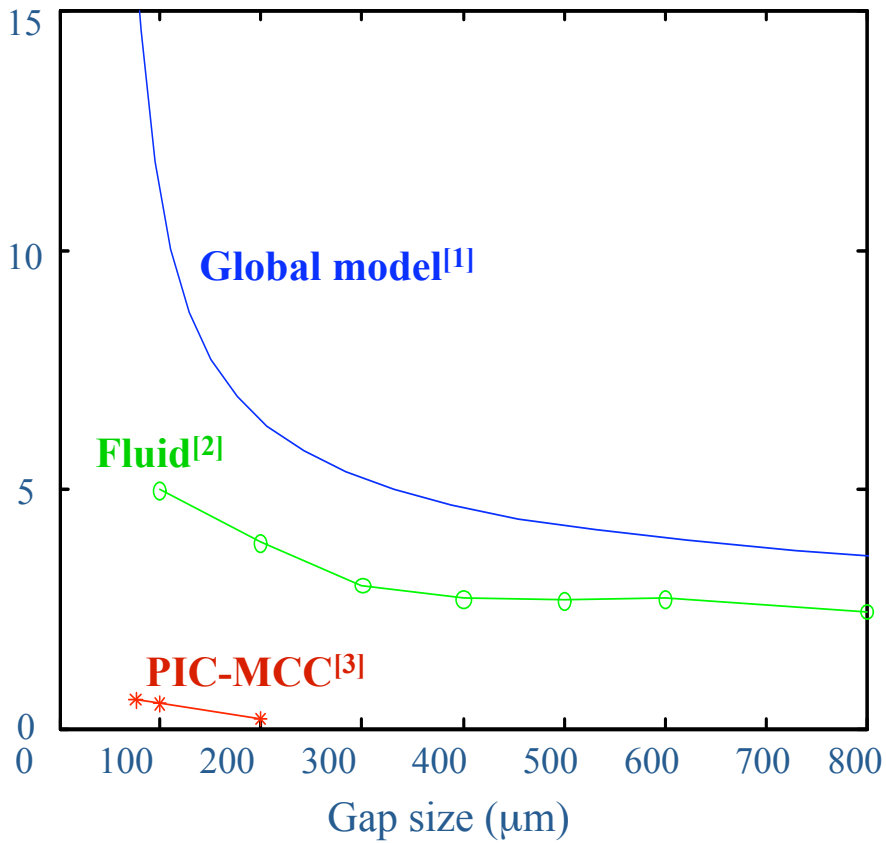

Global model:

$$n_g K_{iz} = \mu_i \frac{kT_e}{q}\left(\frac{1}{\Lambda}\right)^2 \quad \text{where } \Lambda = \frac{L}{\pi}$$

For Heat 760 Torr :

$$\left.\begin{aligned} E &= 10^4 \frac{V}{m} \Rightarrow \mu_i = 2.9\cdot 10^{-4} \frac{\mathrm{m}^2}{\mathrm{Vsec}} \\ E &= 10^5 \frac{V}{m} \Rightarrow \mu_i = 2.85\cdot 10^{-4} \frac{\mathrm{m}^2}{\mathrm{Vsec}} \\ E &= 10^6 \frac{V}{m} \Rightarrow \mu_i = 2.26\cdot 10^{-4} \frac{\mathrm{m}^2}{\mathrm{Vsec}} \end{aligned}\right\} \mu_i \approx 2.5\cdot 10^{-4} \frac{\mathrm{m}^2}{\mathrm{Vsec}}$$

Mobility data obtained by PIC-MCC simulation

K_{iz} is obtained numerically with the cross section data used in the PIC simulation and assuming a Maxwellian electron energy distribution function.

[1] M. A. Lieberman and A. J. Lichtenberg, *Principles of Plasma Discharges*, 2nd ed. (John Wiley & Sons Inc., 2005)
[2] J. J. Shi and M. G. Kong, Physical Review Letters **96**, 105009 (2006)
[3] F. Iza, J. K. Lee, and M. G. Kong, Physical Review Letters **99**, 075004 (2007)

POSTECH

Modeling of Plasma Kinetics via PIC

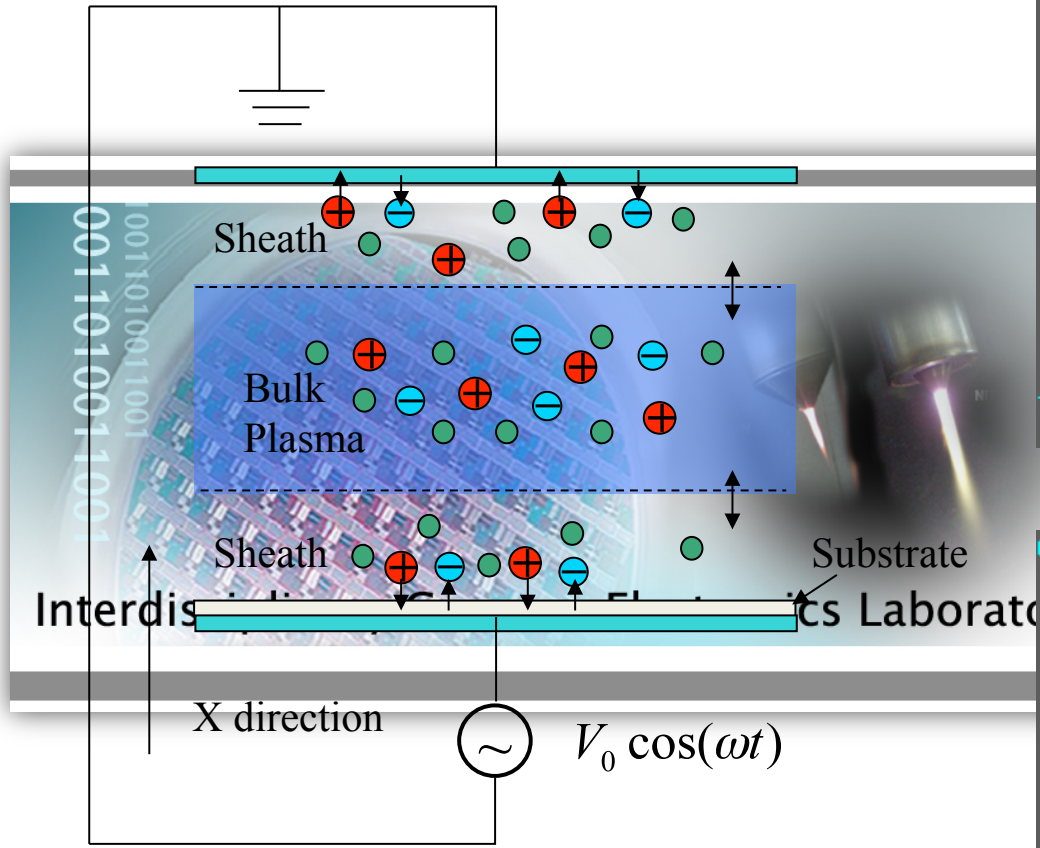

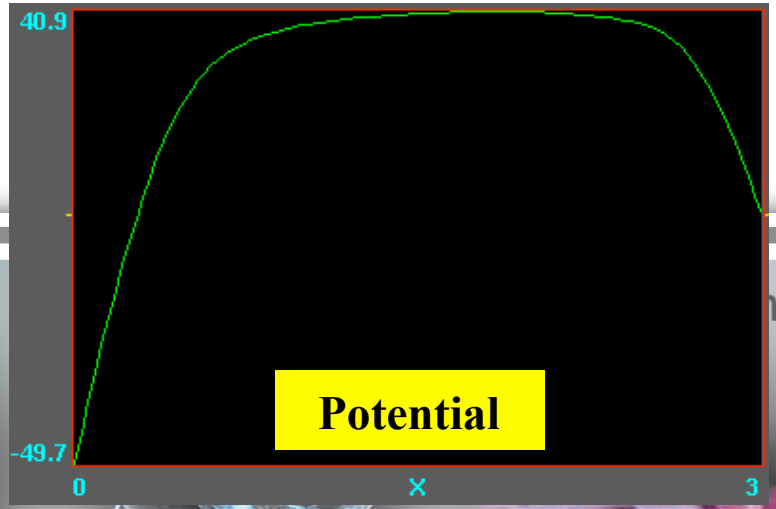

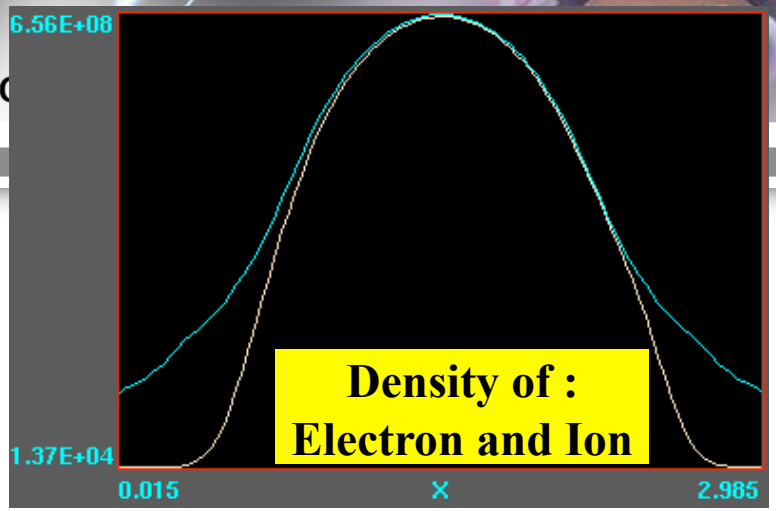

- 1D RF Voltage-Driven System

Basic concept of N_D

Plasma properties with N_D♪

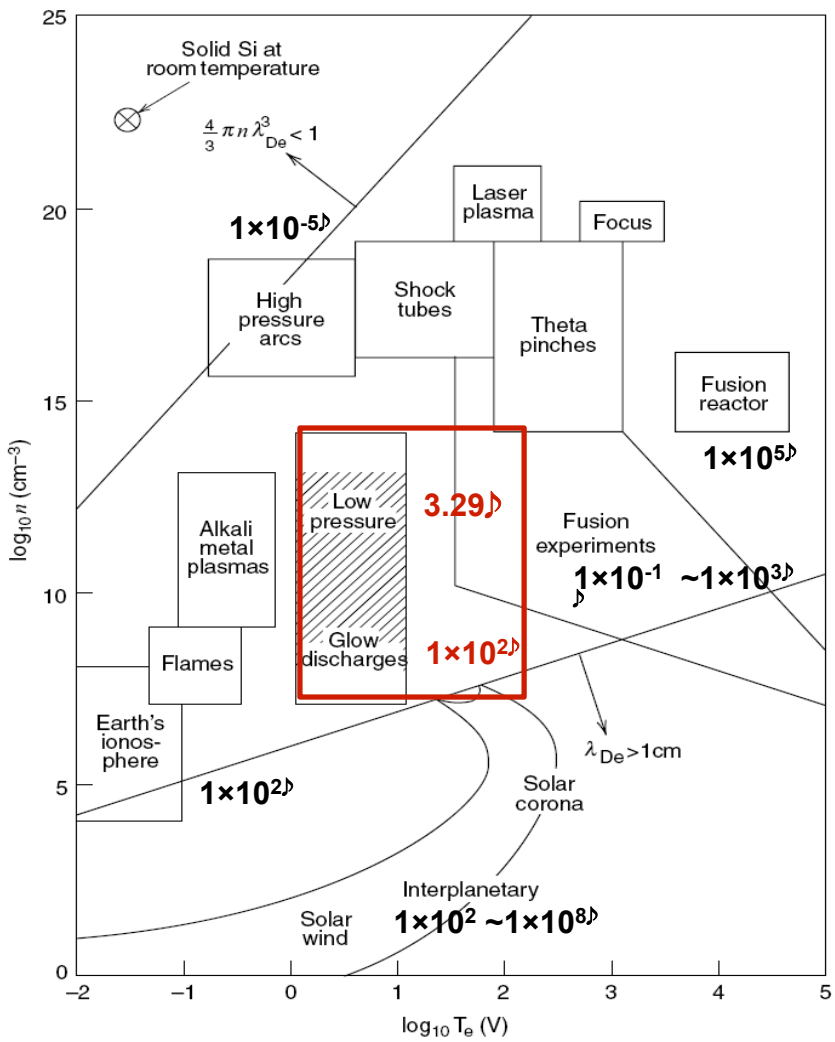

Description	Plasma parameter magnitude	
	Λ<<1	Λ>>1
Coupling	Strongly coupled plasma	Weakly coupled plasma
Debye sphere	Sparsely populated	Densely populated
Electrostatic influence	Almost continuously	Occasional
Typical characteristic	Cold and dense	Hot and diffuse
Examples	Solid-density laser ablation plasmas Very "cold" "high pressure" arc discharge Inertial fusion experiments White dwarfs / neutron stars atmospheres	Ionospheric physics Magnetic fusion devices Space plasma physics Plasma ball

- Each N_D is estimated based on the eq. (1)
- N_D in Low pressure and glow discharge region is about 1~10^2

$$N_D = \frac{(\varepsilon_0 k T_e)^{3/2}}{q_e^3 n_e^{1/2}} \quad \text{equation (1)♪}$$

POSTECH

Basic concept of N_D

- **Physical definition of Debye number in 3D**

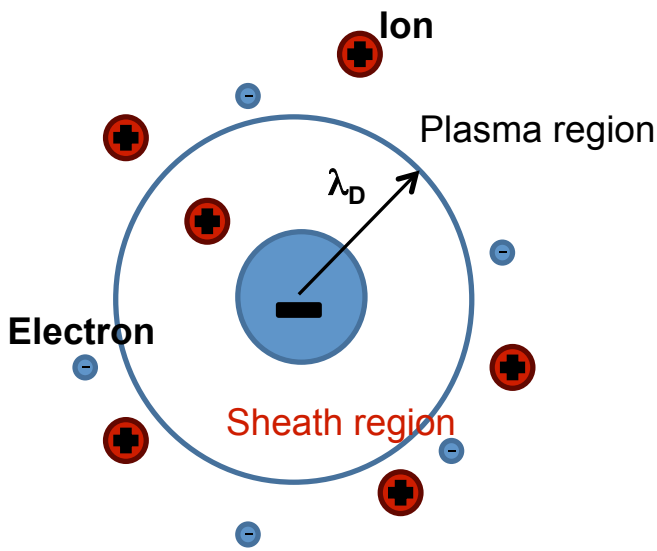

Substitution

$$N_D = \frac{4\pi}{3} n \lambda_D^3 \Leftarrow \lambda_D = \sqrt{\frac{\varepsilon_0 k T_e}{n_e q_e^2}} \approx 743\sqrt{\frac{T_e}{n_e}}(cm)$$

$$\therefore N_D = \frac{(\varepsilon_0 k T_e)^{3/2}}{q_e^3 n_e^{1/2}}$$

- **Definition of Debye number at the 1D PIC simulation**

Debye number (N_D) in **1D PIC simulation** can be defined as a <u>number of particle per Debye length (λ_D)</u>

POSTECH

ICNSP (2009)

K3

PIC-MCC (Particle In Cell with Monte Carlo Collisions) simulations of low temperature plasm

M. M. Turner

School of Physical Sciences and National Centre for Plasma Science and Technology, Dul City University, Ireland

The particle-in-cell method is a classical approach to plasma simulation. though this technique first appeared more than forty years ago, it remains preferred approach for many problems where a kinetic treatment is desi This is especially true in low-temperature plasma physics, where violei non-Maxwellian electron energy distributions are common, often featu bumps, holes and other curious structures. Such complicated distribut functions are typically formed by a subtle interplay between collisional eff and non-local interactions with electric and magnetic fields. It is importan get this right in a simulation, because the electron energy distribution fu tion affects the ionization rate, transport processes, radiative processes, These parameters are of great importance in low-temperature plasma ap cations, which motivate much work in this field. Consequently, one want have a simulation method that in principle captures these effects accurat As a direct solution of the coupled system of the Boltzmann equation Maxwell's equations, particle-in-cell simulation combined with Monte Ca collisions is such a method. This approach should capture the physics curately, provided that the numerical parameters are properly chosen. numerical parameters in question are three: the time step Δt, the cell size and the number of super-particles per cell, N_C. The literature contains v ous heuristics for choosing these parameters, and it is usually assumed t these heuristics apply whether or not Monte Carlo collisions are em- ploy We will show here that this is not always so—Monte Carlo collisions in change the kinetic properties of a particle-in-cell simulation, such that the of numerical thermalisation may increase by orders of magnitude. This is turn means that numerical effects may distort the electron energy distribut function (in particular) to a much greater extent than is often realised. Th effects means that new heuristics are needed, especially for choosing the nu ber of particles. We will discuss the implications of these results.

JPD (2005)

to be considered [16, 38]. The cell size should generally be smaller than the shortest characteristic length scale of the plasma, i.e. Debye length, sheath length and Larmor radius. The time step should generally be smaller than the shortest characteristic time scale of the plasma, i.e. inverse of plasma frequency, RF driving frequency and maximum collision frequency. The particle Courant condition $v\Delta t/\Delta x < 1$, where v is the particle velocity, should also be satisfied for all particles. And an additional constraint in PIC-MCC simulations is imposed by the statistical description of collisional processes. The time step generally needs to be kept small enough to prevent particles from undergoing more than one collision in one time step. This requirement is satisfied if $\Delta t \nu_{max} \ll 1$ where ν_{max} is the maximum collision frequency of the particles. In order to obtain meaningful results at steady state, simulations for RF discharges are typically run for several thousands of RF cycles requiring long simulation runs.

2.2.2. Strengths and limitations. The major limitation of PIC-MCC simulations is the computation time. This is proportional to the number of super-particles and it is therefore desirable to keep the number of super-particles as low as possible. A number of issues, however, need to be considered when selecting the number of super-particles.

(1) Sufficient statistical representation of energetic particles: for example, in a Maxwellian distribution of 2 eV the number of particles with 20 eV is four orders of magnitude lower than the number of particles with 2 eV. Therefore, a sufficiently large number of particles needs to be simulated to properly represent processes that involve high-energy particles, such as excitation and ionization processes.

(2) Noise: since the plasma behaviour is modelled by simulating a reduced number of computer particles (N), PIC-MCC simulations are intrinsically noisy. The noise is inversely proportional to the square root of N. There is, however, a practical limitation on noise reduction that can be achieved by increasing the number of super-particles. Some alternative techniques such as high frequency or short wavelength filtering have been developed to reduce the noise level [2]. In this case, however, one needs to pay attention to the kind of physics that may also be filtered.

(3) Numerical heating: particles may gain or lose energy due to the numerical heating associated with the noise level in the simulation [39, 40]. A sufficiently large number of particles is needed to keep this non-physical energy exchange negligible during the duration of the simulation. As a compromise between numerical accuracy and computational speed, the number of super-particles per cell is typically kept between a few particles up to hundreds of particles. However, when particles in the discharge are trapped for long periods of time, thousands of particles per cell may be required to prevent numerical heating. Figure 2 shows the electron density and temperature in an argon capacitively coupled discharge as a function of the number of super-particles per cell obtained from a one-dimensional PIC-MCC simulation [41] using XPDC1 [16, 19, 20]. Since the electric field in the bulk plasma where low-energy electrons are confined for a long time is small, numerical fluctuations in the electric field value lead

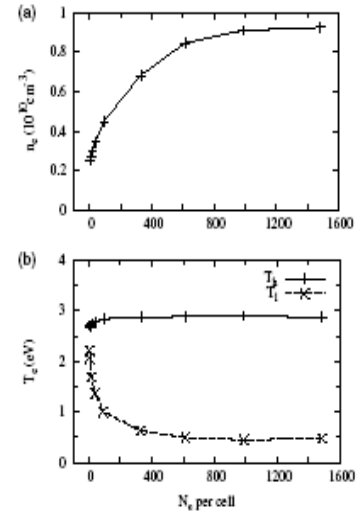

Figure 2. (*a*) Electron density and (*b*) electron temperatures in the bulk plasma as a function of the number of super-particles in a cell. T_h and T_l represent the effective temperatures of high- and low-energy electrons, respectively.

to a significant non-physical heating of low-energy electrons. These fluctuations, however, have a less marked effect on high-energy electrons, which are mainly heated in the sheaths where large electric fields exist. For the case shown, it can be seen that over a thousand super-particles per cell are needed to minimize this numerical artefact.

Due to these constraints on the number of super-particles, PIC-MCC simulations are computationally more demanding than fluid simulations. The large number of particles needed to simulate each species limits in practice the number of species that can be modelled. For this reason, PIC-MCC simulations are normally not used when simulating low-temperature discharges with complex chemistry that involves numerous species. Nevertheless, since fundamental equations are solved with few approximations, kinetics of the simulated species can be accurately modelled, including both local and non-local effects. Therefore, PIC simulations are well suited for low pressure discharges where non-local effects can be very important, particle densities are low and the MCC scheme can be solved relatively quickly.

Finally, it should be mentioned that various techniques have been developed to speed up PIC-MCC simulations. These techniques include implicit movers, longer ion time steps, lighter mass ions, different weights for electrons and ions, non-uniform initial density profiles, different weights for low- and high-energy particles and code parallelization [38, 42, 43]. Although simulation time can be drastically reduced in some cases by a combination of these techniques, PIC-MCC codes remain typically slower than fluid codes.

Other references

The electron density and electron temperature for the different numbers of super-particles

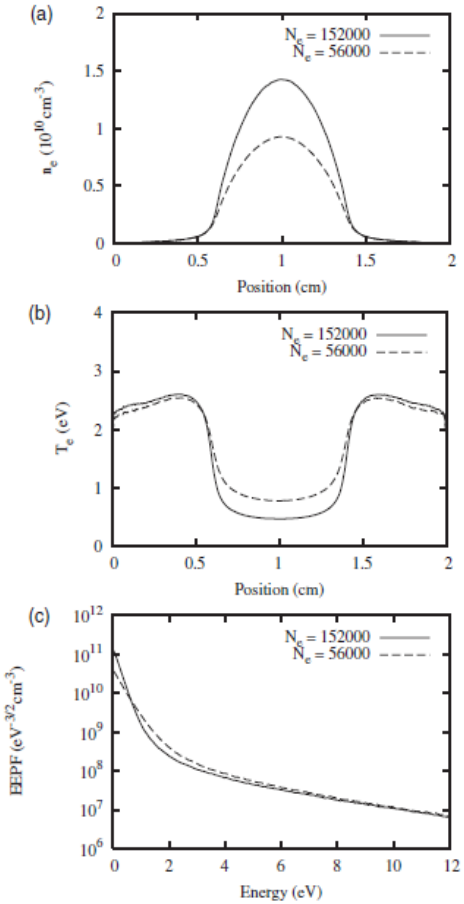

Fig. 3. The spatial profiles of (a) electron density and (b) electron temperature for different numbers of superparticles. (c) The EEPFs obtained at the discharge center for different numbers of superparticles. N_e represents the total number of superparticles for electrons in the system.

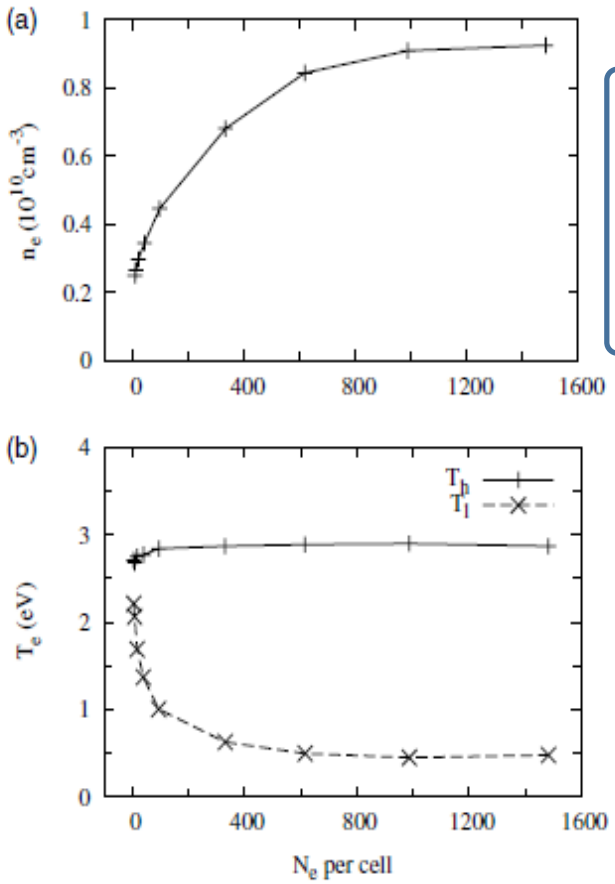

Figure 2. (*a*) Electron density and (*b*) electron temperatures in the bulk plasma as a function of the number of super-particles in a cell. T_h and T_l represent the effective temperatures of high- and low-energy electrons, respectively.

- Condition
  - ✓ Gas : Ar
  - ✓ Gap : 2cm
  - ✓ Current : 2.65mA/cm2
  - ✓ Frequency : 13.56MHz
  - ✓ Pressure : **100mTorr**

POSTECH

Ref.] H.C. Kim, F. Iza, S.S. Yang, M. Radmilovic-Radjenovic, and J.K. Lee, J. Phys. D: Appl. Phys. 38 R283-R301 (2005)

Other references

- Condition
  - ✓ Gas : Ar
  - ✓ Gap : 2cm
  - ✓ Current : 30A/m2
  - ✓ Frequency : 13.56MHz
  - ✓ Pressure : **100mTorr**

- Density

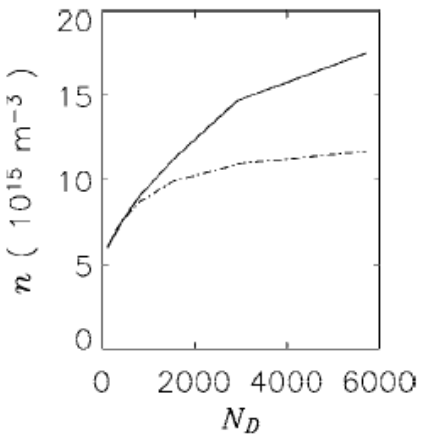

FIG. 6. Plasma density at the discharge midplane, as a function of the number of simulation particles per Debye length, for a radio frequency discharge in argon, with plane electrodes separated by 2 cm, an excitation frequency of 13.56 MHz, a pressure of 100 mTorr and a current density of 30 A m^{-2}. Result without electron-electron collisions (solid line) and the corresponding result with electron-electron collisions (dashed line).

- Effective electron temperature

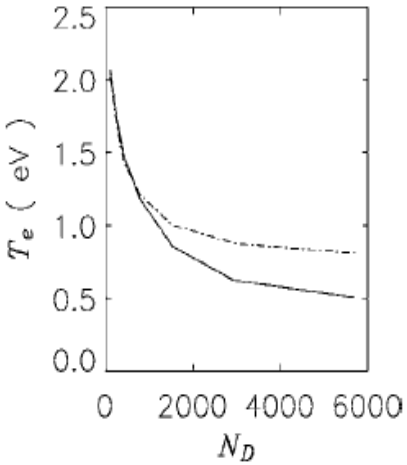

FIG. 7. Effective electron temperature at the discharge midplane, for a radio frequency discharge at the conditions and with the rubric of Fig. 6.

- EEPF

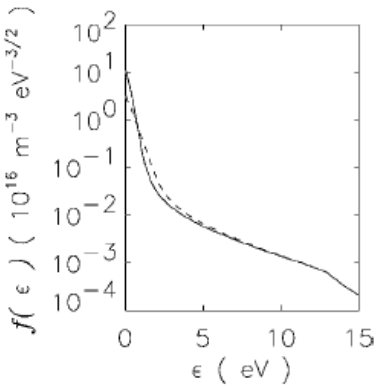

FIG. 8. Electron energy distributions at the discharge midplane, for the discharge conditions of Fig. 6. Both curves are for $N_D \simeq 6000$. Calculations excluding (solid curve) and including (dashed curve) electron-electron collisions. The temperatures of the low energy groups of electrons are approximately 0.25 eV for the case without electron-electron collisions and 0.49 eV with electron-electron collisions.

Ref.] M. M. Turner, PHYSICS OF PLASMAS 13, 033506 2006

Relation between N_D and N_C

nc2p variation ➔ N_C and N_D variation

nc2p	N_c	N_d
6.00E+09	2.67E+02	1653.3
4.00E+09	4.00E+02	2420
3.50E+09	4.57E+02	2742.85
2.50E+09	6.40E+02	3840
2.00E+09	8.00E+02	4760
1.50E+09	1.07E+03	6346.6
9.00E+08	1.78E+03	10488.8

Computational Number

$$N_C = \text{initn} \cdot A \cdot L / \text{nc2p} \cdot \text{grid \#}$$

$$= \text{initn} \cdot A \cdot \Delta X \ / \ \text{nc2p}$$ ← L / grid

= ΔX

Physical Number

$$N_D = \text{initn} \cdot A \cdot \lambda_D \ / \ \text{nc2p}$$

Debye number (N_D) in **1D PIC simulation** can be defined as a <u>number of particle per Debye length (λ_D)</u>

Initn : initial electron density
A : area
Nc2p : The number of physical particles per computer particle.

$$N_D \ / \ N_C \approx \lambda_D \ / \ \Delta X$$

POSTECH

Electron Temperature with variations of N_C and N_D

H. C. Kim's case

Ref: J.Phys. D : Appl. Phys. 38 (2005) R 283- R301

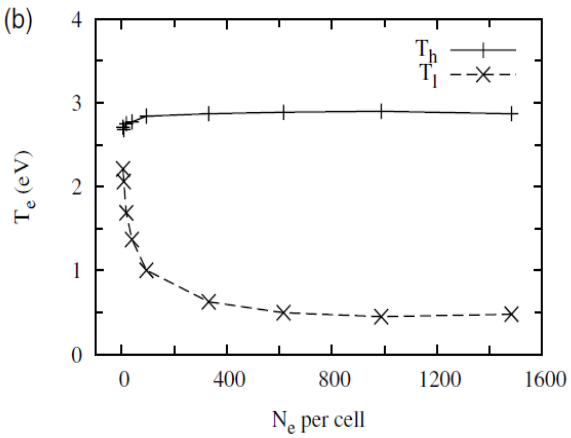

H. Y . Kim's case

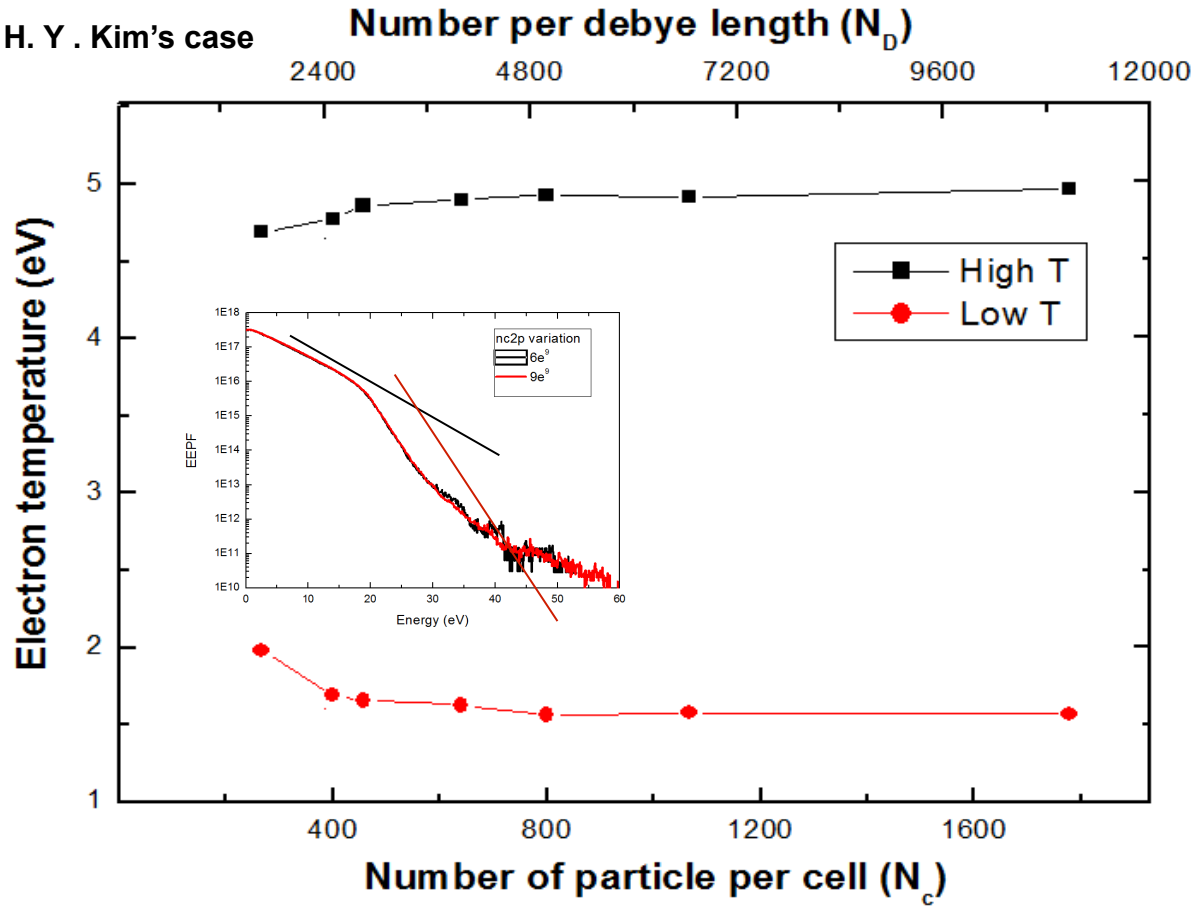

Our Simulation condition

- Gas pressure: **760 Torr**
- Gap size: **200 μm**
- Gas: **Ar**
- Frequency: **500MHz**
- Voltage : 130V
- Grid: **100**
- Area: **0.01 m²**

- Simulation result at the atmospheric pressure shows similar trend with low pressure case (H.C.Kim's case)
- Electron density is starting to saturate after 800 of N_C (≈ 4800 of N_D)

POSTECH

Electron Temperature with variations of N_C and N_D

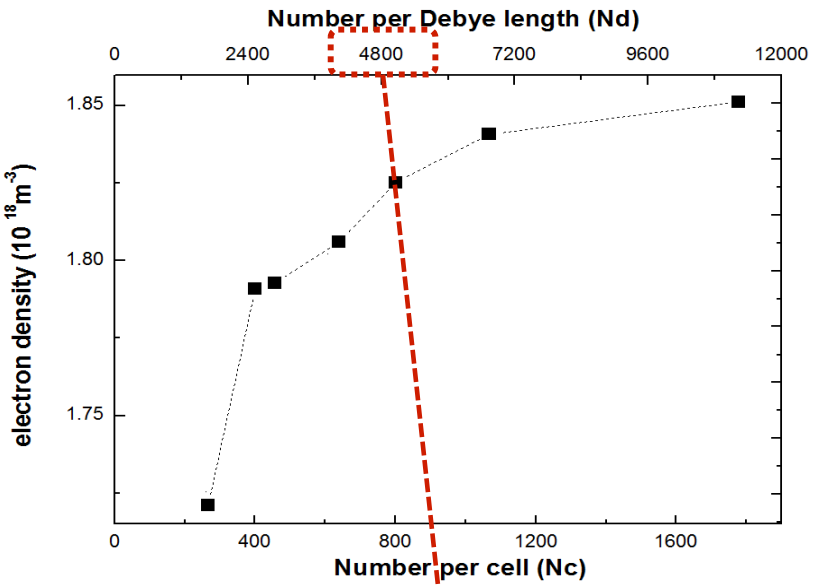

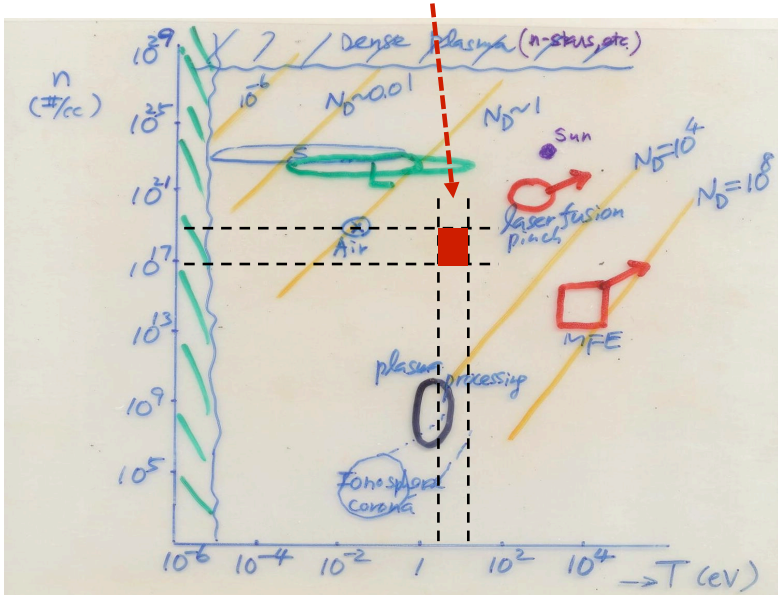

- Value of N_D at where 1D PIC simulation is starting to saturate is on the similar N_D region calculated by saturated electron density and electron temperature
- It can be new standard for selecting N_C for the reliable results from simulation

Selecting the simulation domain on the N_D plane

↓

Take the N_D value on that domain

↓ ← $N_D / N_C \approx \lambda_D / \Delta X$

Get the N_C value using the relation between N_C and N_D

POSTECH

Global modelings of two experiments

➢ Experiment 2

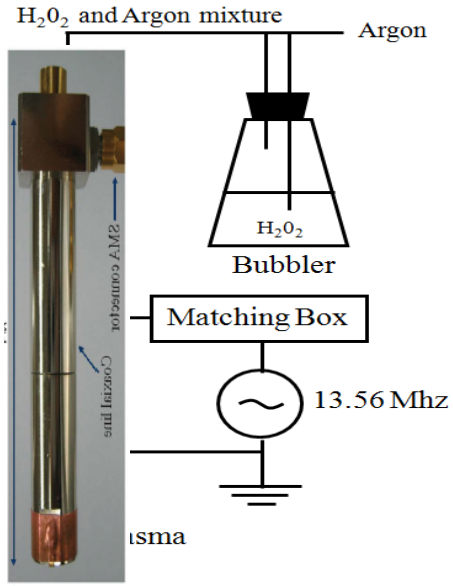

- Experimental condition♪

- Type : Direct treatment
- Gas : H2O2 / Ar
- Pressure : 760 Torr
- Power : 10 W
- Method : H2O2 vapor system

(water concentration is less than 1000 ppm
)

➢ Experiment 1

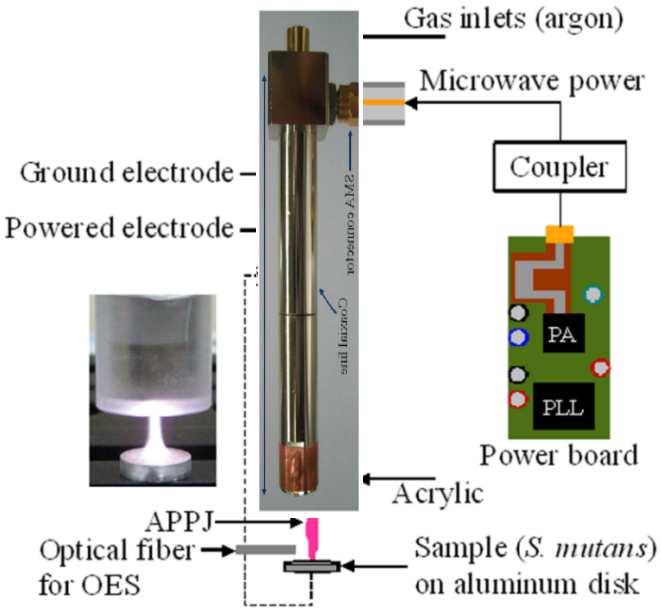

- Experimental condition♪

- Type : Direct treatment
- Gas : H2O2 or H2O / Ar
- Pressure : 760 Torr
- Power : 4 W
- Method : H2O2 or H2O liquid system

(water concentration is more than 1000 ppm)

Global Model: Particle and Energy Balance in Discharges

Uniform density discharge model

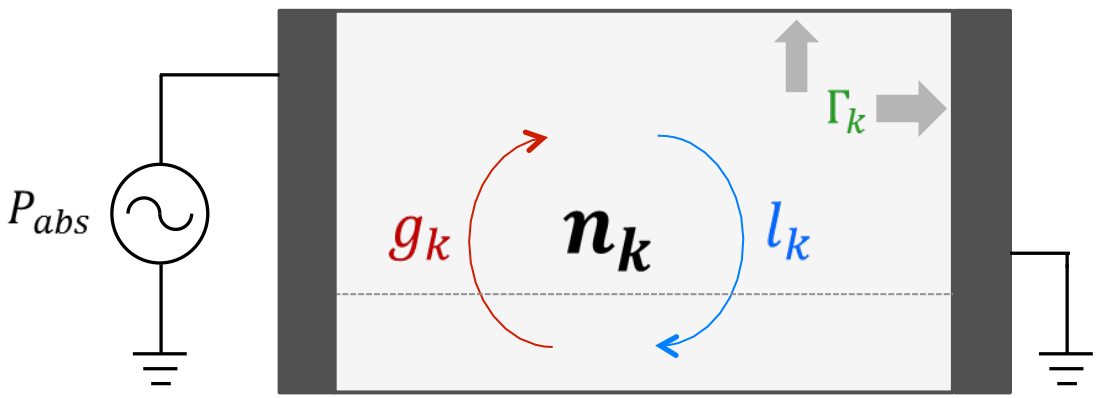

n_k : Density of species k (cm^{-3})

g_k : Generation rate due to the chemical reactions

l_k : Loss rate due to the chemical reactions

Γ_k : Flux into the boundary

Particle balance equation♪

$$\frac{d}{dt}(\boldsymbol{n_k}) = [g_k(T_e, T_n) - l_k(T_e, T_n)] - \Gamma_k$$

T_e, T_n : Electron and neutral gas temperature (K)

n_e →

← T_e

Power (or energy) balance equation♪

$$\frac{d}{dt}\left(\frac{3}{2} n_e T_e\right) = P_{abs} - P_e$$

$\frac{3}{2} n_e T_e$: Total energy of species in the discharge

n_e : Electron density

P_{abs} : Input power density

P_e : Power loss of electrons due to the chemical reactions

POSTECH

$Ar/N_2/O_2/H_2O/H_2O_2$ Discharge: 73 Species & 481 Reactions

Input gas (5)		Ar, N_2, O_2, H_2O_2, H_2O
Neutral radicals (29)		Ar*, Ar**, O_2*, O, O*, O_3, O**, O2(A), O2(B), OH, OH(A), H, H_2, H (2), H(3), HO_2, NO, N, NH, HNO, NH_2, NH_3, N_2H_2, N_2H_3, N_2H_4, N NH, NO_2, N_2O, NO_3
Charged sp ecies	Positive (29)	Ar^+, Ar_2^+, O_2^+, O^+, OH^+, H_2^+, H^+, O_4^+, H_3^+, H_2O^+, H_3O^+, $H_5O_2^+$, $H_4O_2^+$, $H_2O_3^+$, $H_7O_3^+$, $H_9O_4^+$, $H_{11}O_5^+$, $H_{13}O_6^+$, $H_{15}O_7^+$, N_4^+, HN_2^+, NO_2^+, N_2^+, NO^+, NH_3^+, NH_4^+, N_3^+, N^+, N_2O^+
	Negative (10)	electron, O_2^-, O^-, O_3^-, OH^-, H^-, NO_2^-, NO_3^-, NO^-, N_2O^-

Table 1. Representative biological roles of the various constituents of LTAPPs.

Constituent	Functional Effects	Ref. No
UV radiation	induces (i) DNA, protein and lipid damages caused by the UV-induced disturbance in the cellular redox state, or (ii) the release of intracellular reactive species.	[2, 74–76]
Charged particles	cause a rupture of the outer membrane of cells by electrostatic force caused by accumulated charges on the outer surface of the cell membrane.	[77–80]
Reactive species:		
NO	offers anti-microbial and anti-tumour defense and is concerned in a multitude of biological activities such as fibroblast proliferation, regulation of immune system, early apoptosis and neural communication.	[1, 20, 81–84]
O_3	has germicidal effects caused by interference with cellular respiration.	[81]
OH	is extremely reactive and can damage virtually all types of macromocules such as lipid and amino acids in proteins.	[81]
O_2^-	is biologically toxic and is concerned in a large number of cell signalling pathways.	[85–88]

Ref: H. W. Lee *et al.*, *J. Phys. D: Appl. Phys.* **44** (2011), 053001

POSTECH

Case 1 : Ar discharge with Submerged Sample

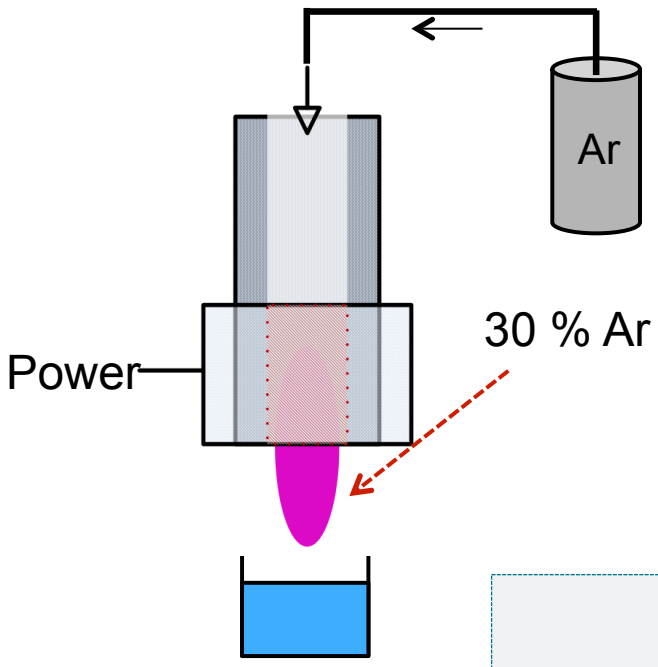

30 % Ar + 70 % Liquid solution

Liquid solution
(**x % H_2O_2** + (1-x) % water)

Simulation Condition

- Gas temperature: 300 K
- Pressure: 1 atm (= 760 Torr)
- Relative humidity: **25 % (+70 %)**
- Gas content
  : Ar + 3% H_2O_2 (+97% water)= **99 %**
  Humid air = **1 %**
  (0.77% N_2 + 0.22% O_2 + **0.008% H_2O**)
- Electron density: 3×10^{11} cm^{-3}

Gas content in the simulation

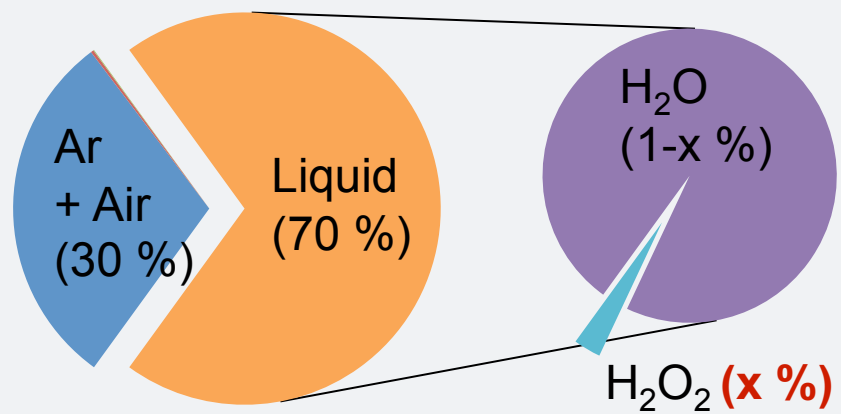

POSTECH

Case 1 : Ar discharge with Submerged Sample

Experimental results

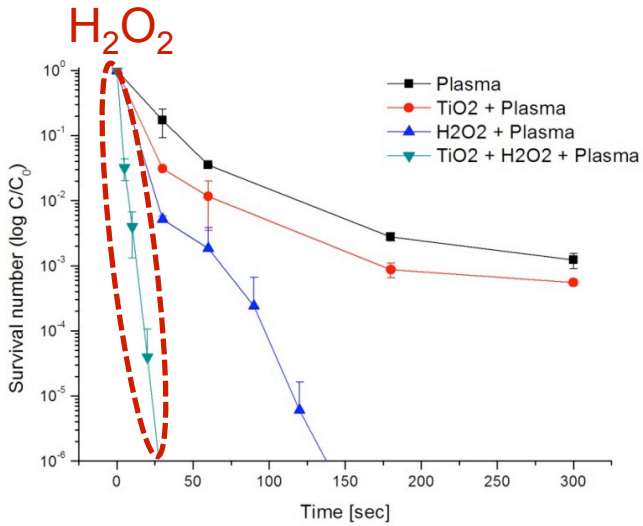

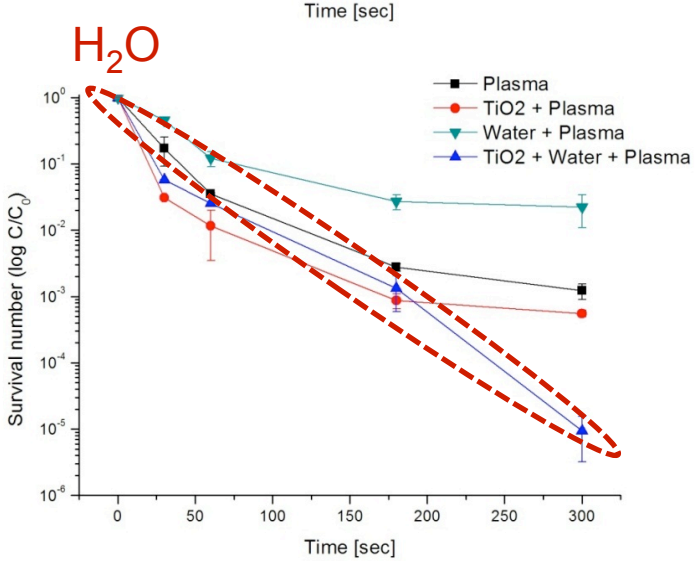

GMoo result

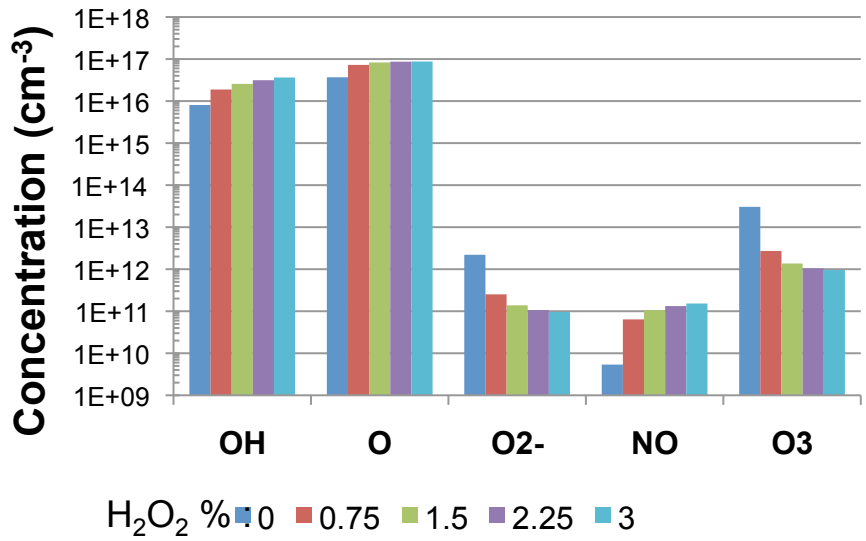

- As H_2O_2 increases, OH, O and NO increase, while O_2^- and O_3 decrease.
- O_3 reduction by X30 with 3 % H_2O_2

POSTECH

Case 1 : 3% H_2O_2 vs. Water (Result of GMoo Simulation)

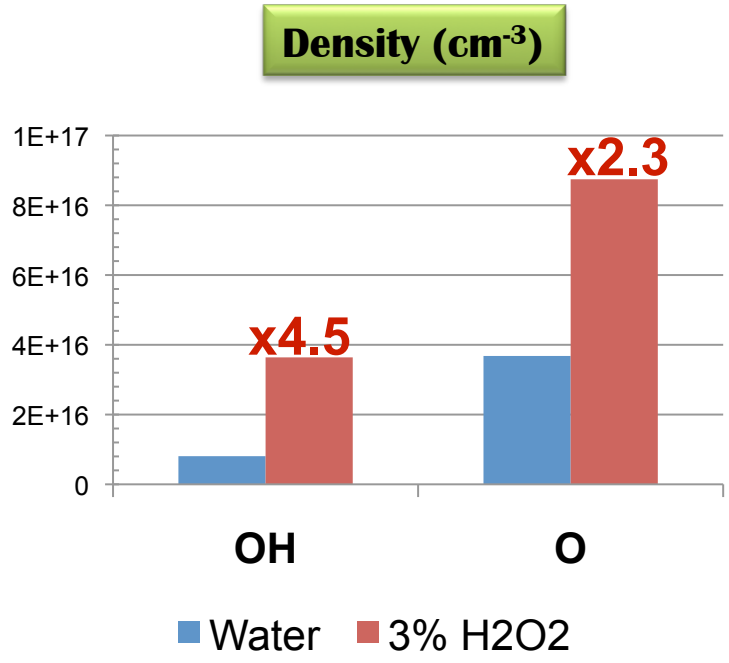

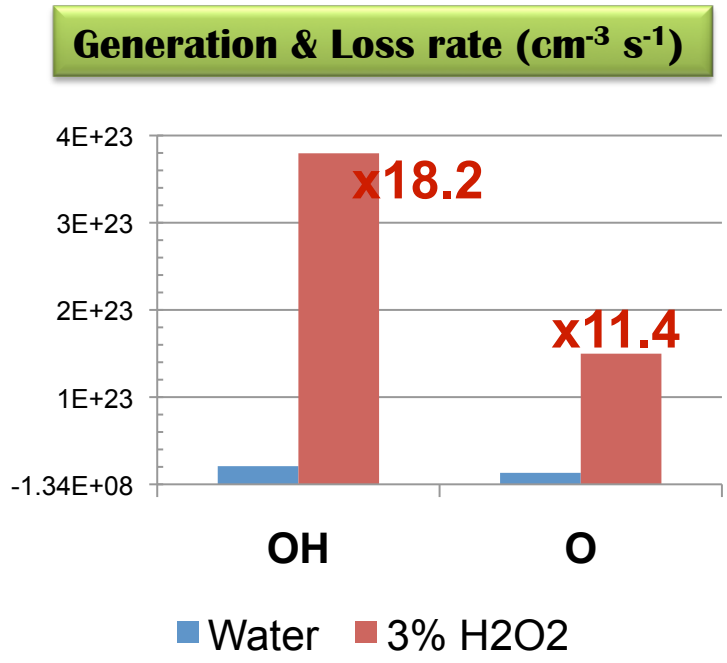

- The 3% of H_2O_2 case shows higher densities of OH and O, and their generation (and loss) rates by X 11-18 than those of water case.
- This might explain the higher sterilization rate with H_2O_2 than H_2O, t hat had been observed experimentally.

POSTECH

Case 2 : Ar discharge in Humid Air + H_2O_2 Bubbler

(1-x) % Ar + **x % Liquid solution** (**3% H_2O_2** + 97% water *or* 100 % water)

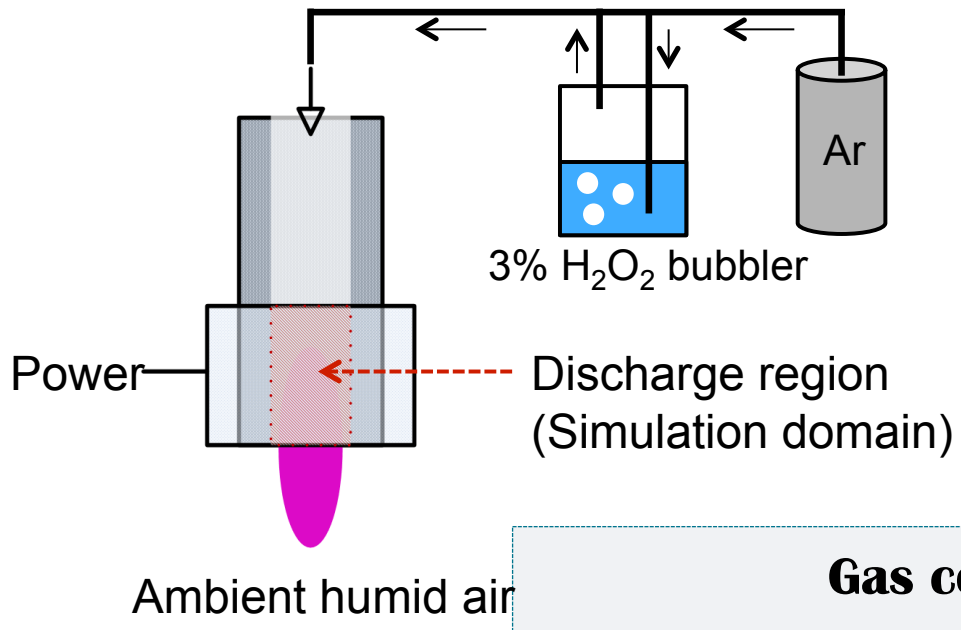

Simulation Condition

- Gas temperature: 300 K
- Pressure: 1 atm (= 760 Torr)
- Relative humidity: **25 % (+70 %)**
- Gas content
  : Ar + 3% H_2O_2 (+97% water)= **99 %**
  Humid air = **1 %**
  (0.77% N_2 + 0.22% O_2 + **0.008% H_2O**)
- Electron density: 3×10^{11} cm^{-3}

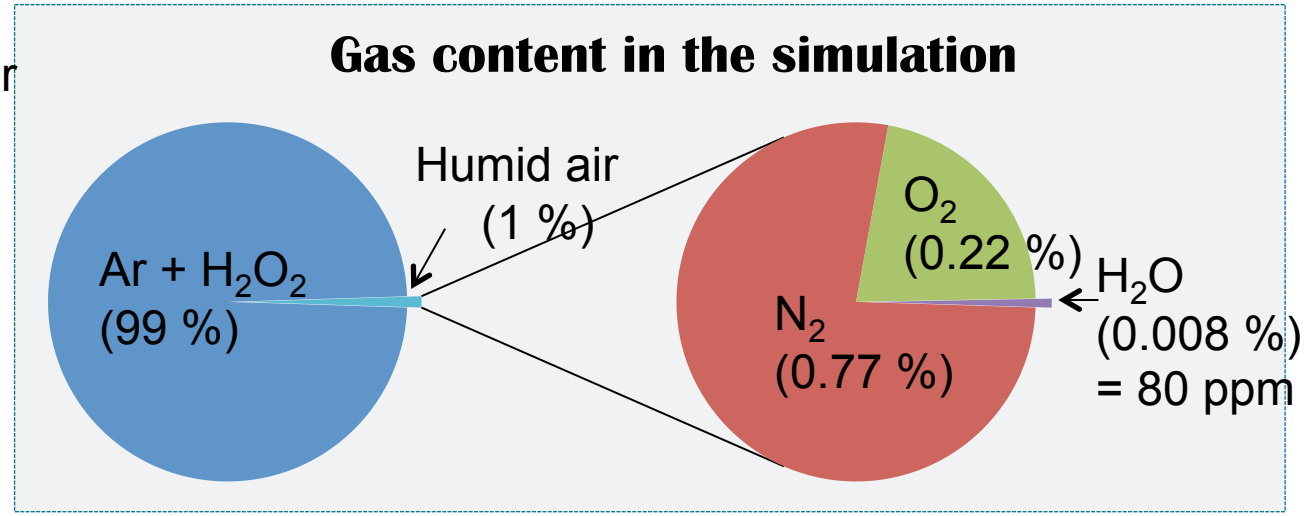

POSTECH

Case 2 : OH and O density: Experiments *vs.* GMoo

[Experimental measurement]

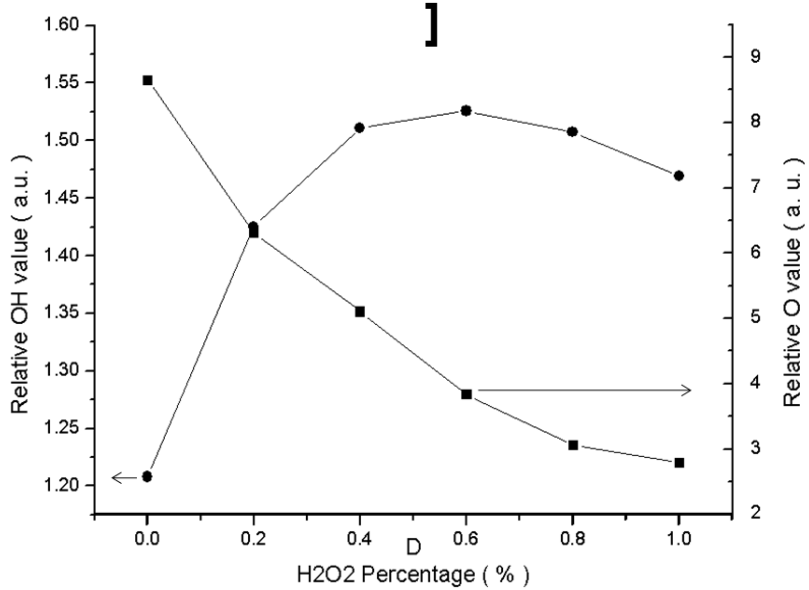

[GMoo]

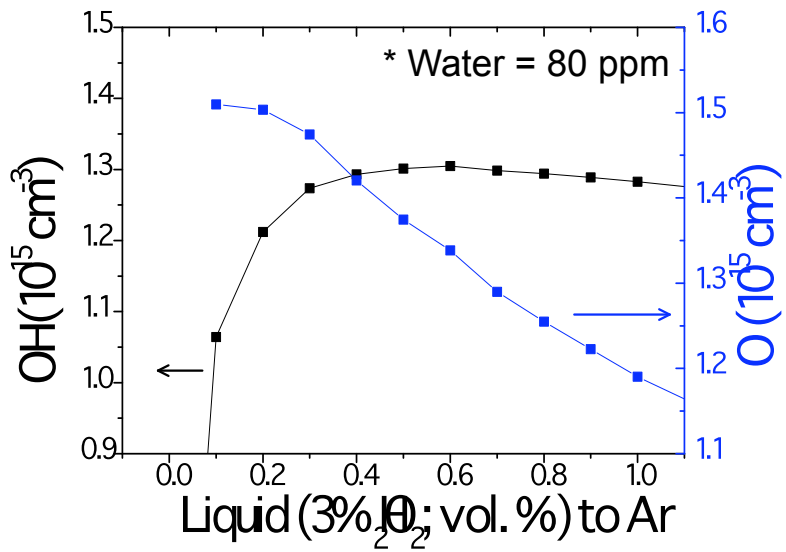

- Result of GMoo shows good agreement with the experimental measurement.
- OH density shows its maximum value at 0.6 % of H_2O_2.
- O density decrease as H_2O_2 concentration increases.

POSTECH

Case 2 : H_2O_2 + H_2O Plasma vs. H_2O Plasma: OH Density

Result of GMoo

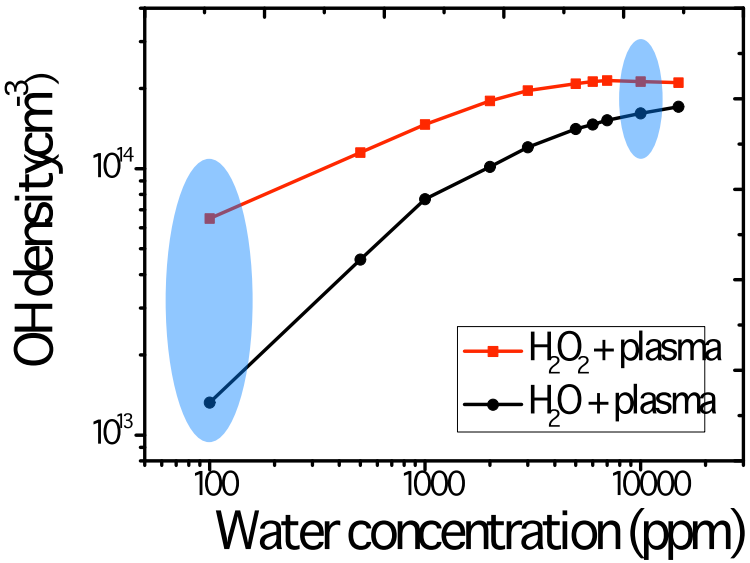

Ratio of OH density

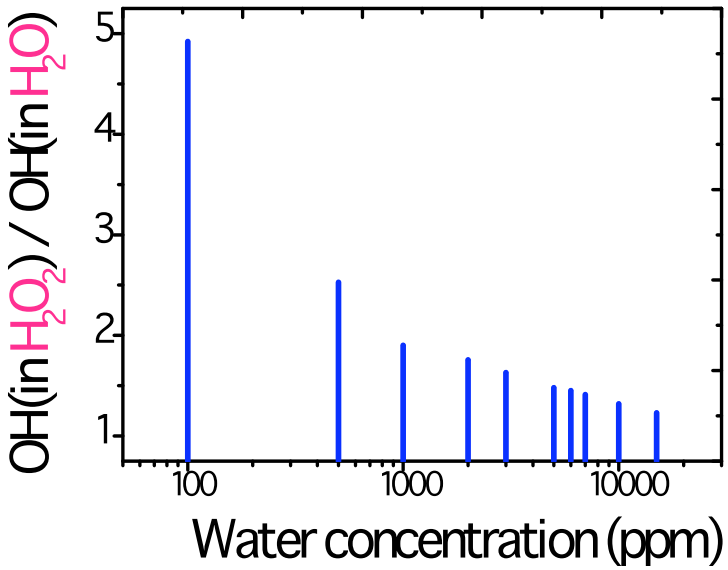

5 times (H_2O_2 + plasma > H_2O + plasma) ♪

- When the water concentration is 100 ppm, OH density in H_2O_2 plasma is five times higher than that in H_2O plasma. This difference is because H_2O_2 is the main source of OH generation.
- As the water concentration increases, the ratio of OH density in H_2O_2 plasma to that in H_2O plasma decreases.

POSTECH

Observation

ND/ Nc = 6

λ_D is 6 times higher than ΔX

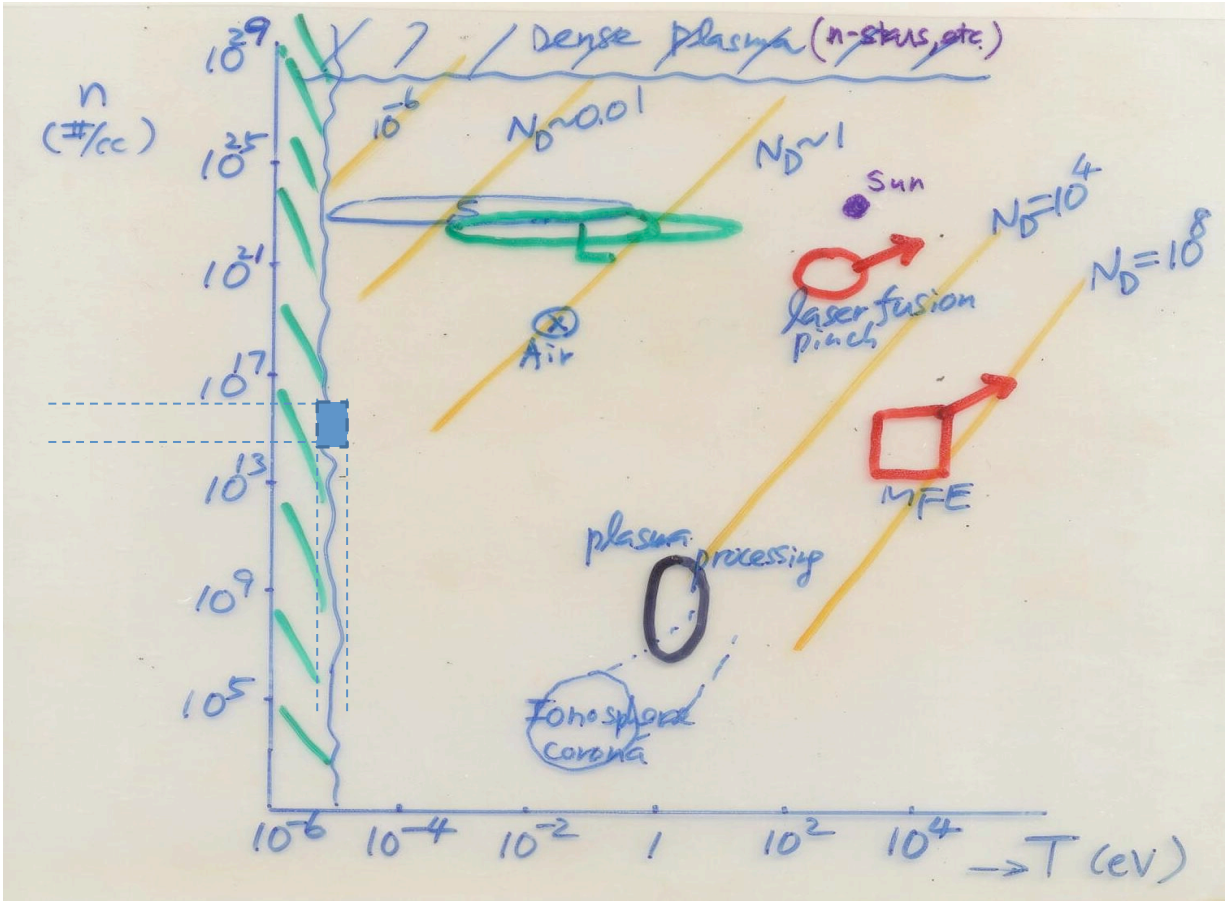

POSTECH

Summary

$N_D / N_C \approx \lambda_D / \Delta X$

- **Advanced version of global model code (GMoo) with a new algorithm has been developed.**
  - Relation table & modularization
    - Easy to add and remove hundreds of species and reactions
    - Usable for other plasmas operated with different gases
  - New algorithm for determining electron temperature (T_e)
    - Remove the power balance equation from the GMoo
    - Advantage: Free from lack of physical information
    - Disadvantage: (1) Need to assume a proper desired electron density($n_{e,desired}$)
      (2) need much longer simulation time
- Ar plasma in humid air with H_2O_2 has been simulated.
  - The decrease of the OH density at the higher concentration of H_2O_2 is due to the drastic increase of OH loss owing to H_2O_2.
  - Higher concentrations of reactive oxygen species in H_2O_2 case might explain the higher sterilization rate with H_2O_2 than H_2O.

Dual-Freq. CCP: Electron Heating Mechanism

- J_h :fixed, 100 mTorrr

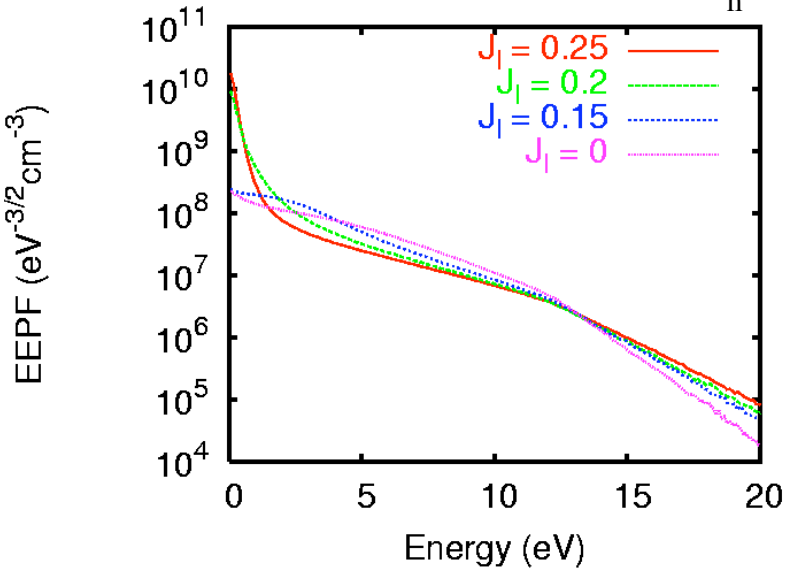

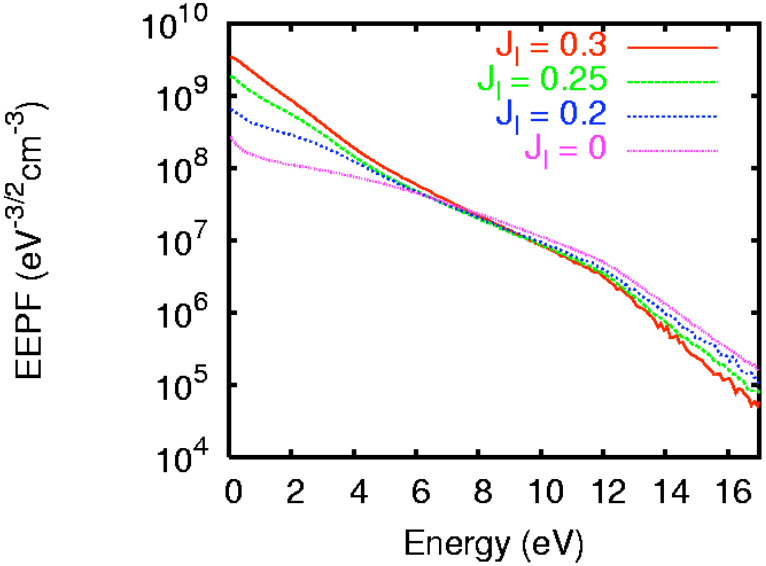

- W/O SEEC :
from collisional (Ohmic) to co llisionless (stochastic)

- With SEEC :
α-γ mode trans ition

✓ Depending on SEEC, the main mechanism for EEDF change differs.

[Ref.] H.C. Kim and J.K. Lee, Phys. Rev. Lett. 93, 085003 (2004).

Electron Bounce Resonance in CCP

- Evolution of EEPF with driving frequency

→ Reflects the Electron Bounce Resonance heating of low-energy electrons with electric field in the bulk, not in the sheath (electron cannot touch the rf sheath)

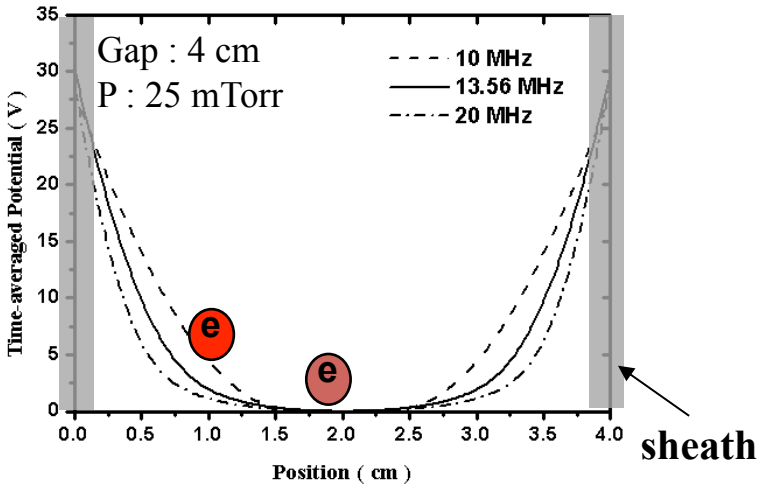

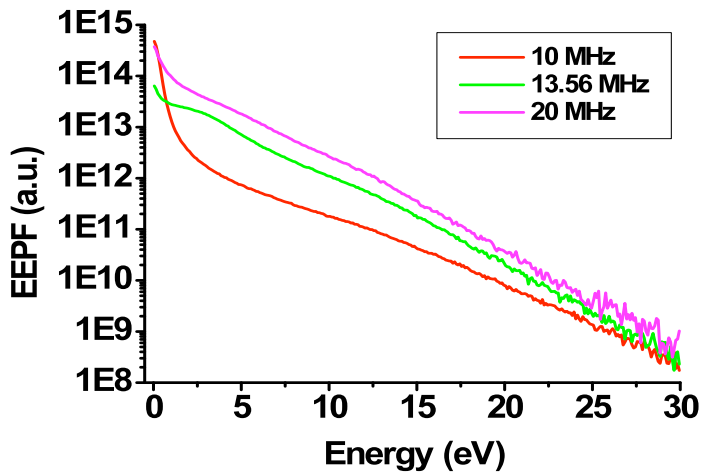

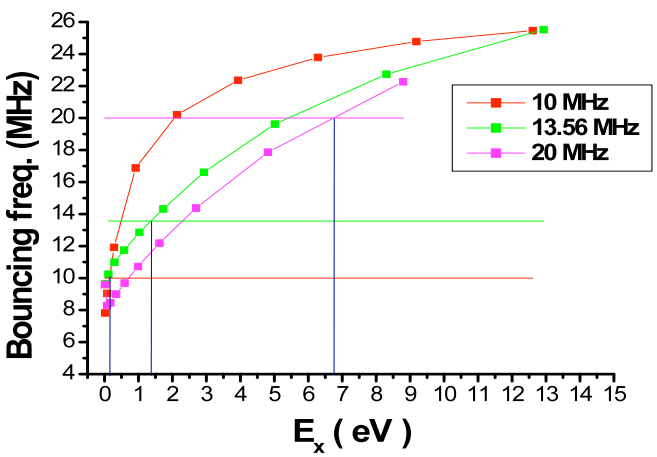

<u>10 MHz</u>: BR heating not observed because the energy gained in one bounce drives the electrons out of resonance.

<u>13.56 MHz</u>: BR heating results in the formation of a plateau in the EEPF for electrons that satisfy $\Omega_{Bounce}(\varepsilon_x) \approx \omega_{rf} / 2\pi$.

<u>20 MHz</u>: BR heating not observed because collisions prevent subsequent coherent interactions with the electric field

[Ref.] G.Y. Park, S.J. You, F. Iza, and J.K. Lee, Phys. Rev. Lett. 98, 085003 (2007).

THANK YOU
FOR YOUR ATTENTION **jkl.postech.ac.kr**

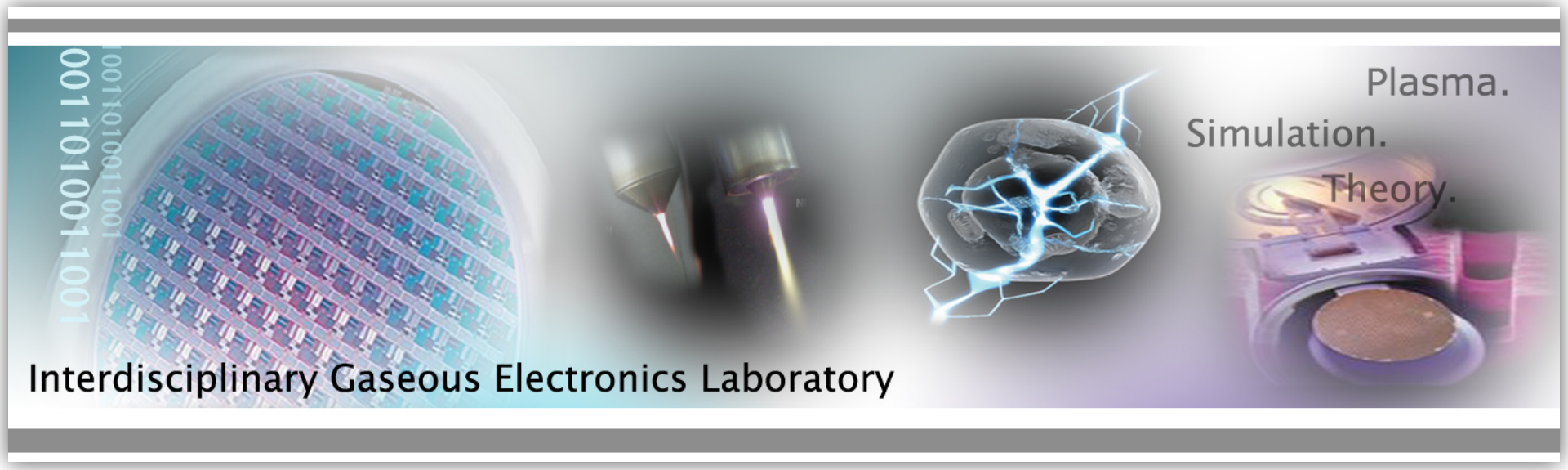

POSTECH

Plasma: Potential and challenge

FUSION PLASMA:
Power generation
Millions of degree K
Size scale: m

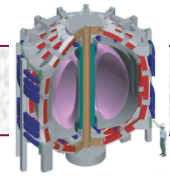

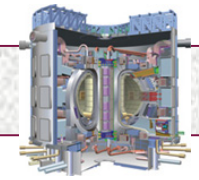

TECHNOLOGICAL PLASMA :
Material processing
Hundreds of degree K
Size scale: cm

HIGH PRESSURE MICROPLASMA:
Biomedical/industrial applications
Room temperature
Size scale: **µm**

The Challenge: Control

Electrical power:
DC, pulsed, DBD, RF, µwave…

Source Configuration:
Electrodes, coils, waveguides,…

Chemistry:
Ar, He, O_2, N_2, NH_3, air, …

Fundamental plasma physics

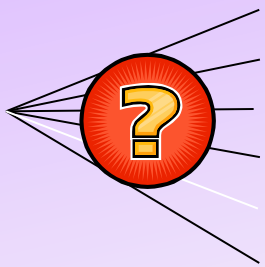

Plasma

Radicals
Ions
Electrons
Photons
Currents
…

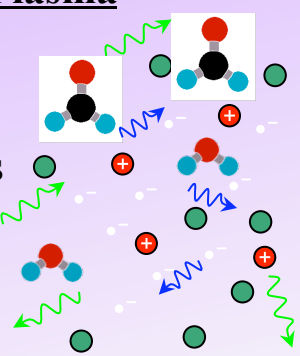

Application specific criteria

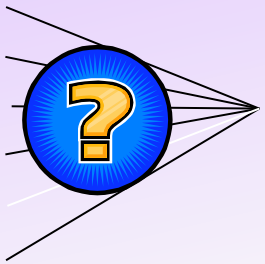

Reactivity
Selectivity
Stability
Efficiency
Lifetime
…

Various plasma techniques → Existing market for medical equipments

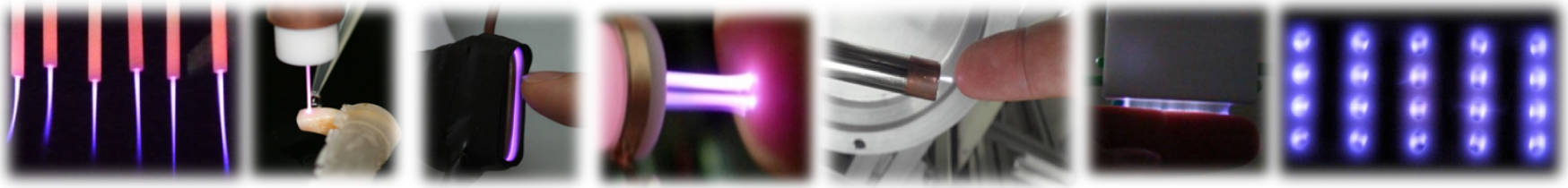

Medical plasma

- Sterilization/disinfection
- Oral care – tooth bleaching
- Skin care
- Wound healing

POSTECH

대기압 플라즈마의 강력한 박테리아 제거

다양한 대기압 플라즈마 제작 가능

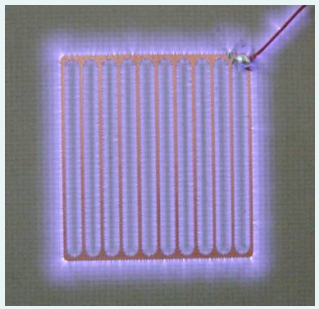

Air Plasma

Ar Plasma

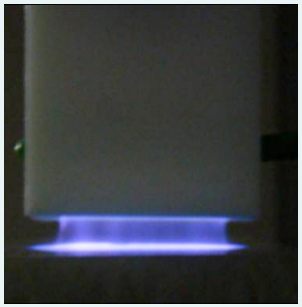

He Plasma

강력한 멸균 특성

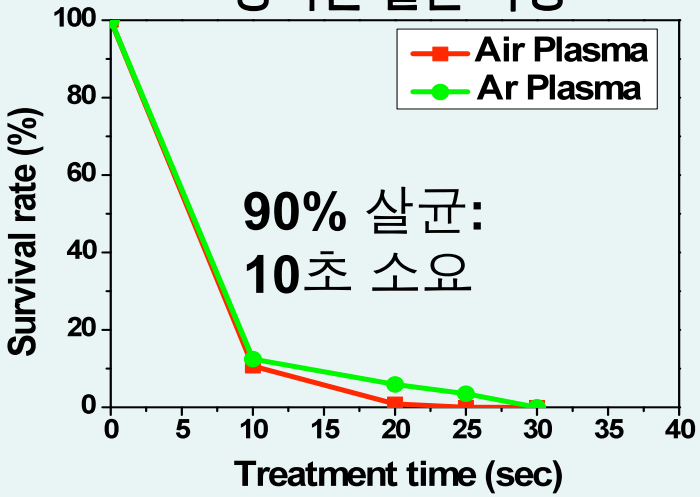

넓은 면적의 살균 효과

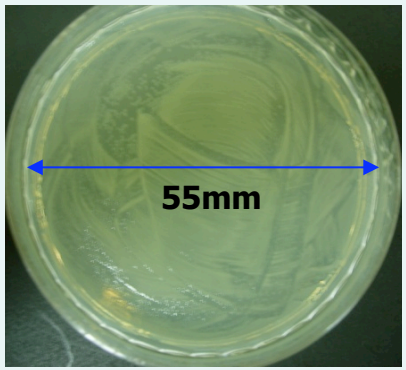

Ar Plasma 처리 전

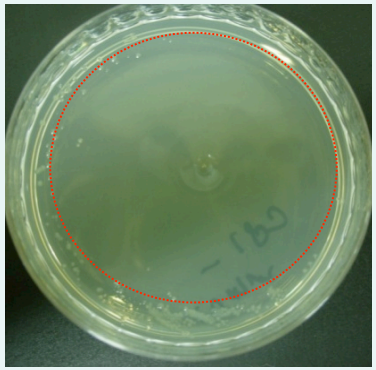

Ar Plasma 처리 후

플라즈마 vs. UV

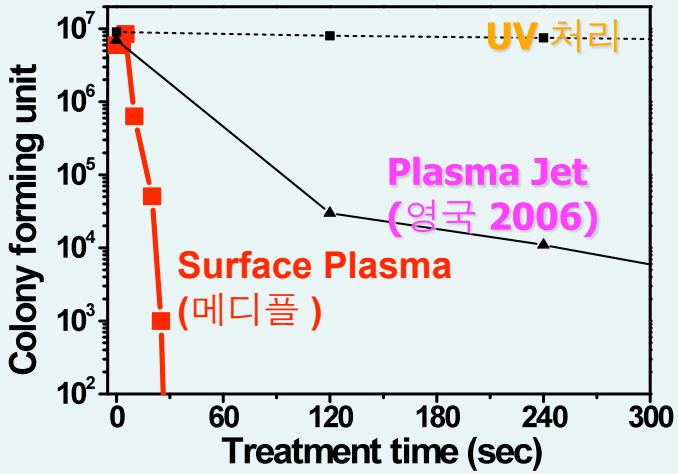

POSTECH

Case 2 : Reactions which are Related to H_2O_2

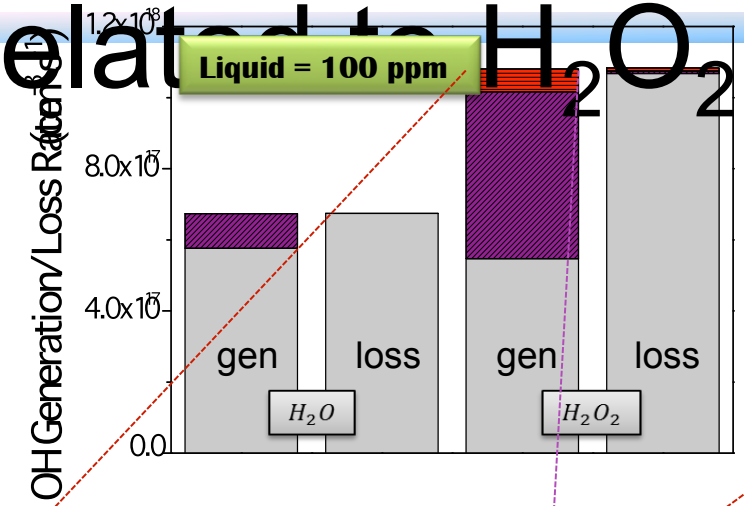

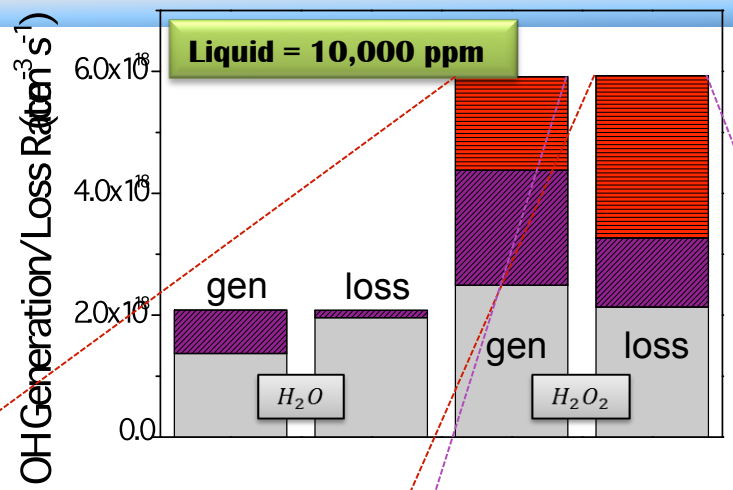

Generation (49.2 %)

Directly related to H_2O_2: **5.9 %**

$O + H_2O_2 \rightarrow OH + HO_2$ (5.3%)
$H + H_2O_2 \rightarrow OH + H_2O$ (0.3%)
$e^- + H_2O_2 \rightarrow e^- + 2OH$ (0.3 %)

Secondary related to H_2O_2: **43.3 %**

$H + HO_2 \rightarrow 2OH$ (23.4 %)
$O + HO_2 \rightarrow O_2 + OH$ (11.0 %)
O_2더A떡 $+ HO_2 \rightarrow O_2 + O + OH$ (8.9 %)

Loss (0.7 %)

Generation (57.3 %)

25.8 %

$O + H_2O_2 \rightarrow OH + HO_2$ (19.8 %)
$e^- + H_2O_2 \rightarrow e^- + 2OH$ (5.8 %)
$e^- + H_2O_2 \rightarrow OH + OH^-$ (0.2 %)

31.5 %

$O + HO_2 \rightarrow O_2 + OH$ (18.9 %)
O_2더A떡 $+ HO_2 \rightarrow O_2 + O + OH$ (6.7 %)
$H + HO_2 \rightarrow 2OH$ (5.9 %)

Loss (64 %)

44.9 %

$OH + H_2O_2 \rightarrow H_2O + HO_2$ (44.9 %)

19.1 %

$OH + HO_2 \rightarrow O_2 + H_2O$ (19.1 %)

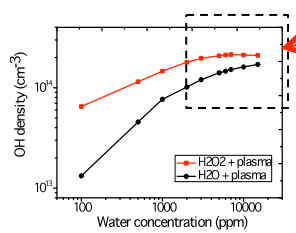

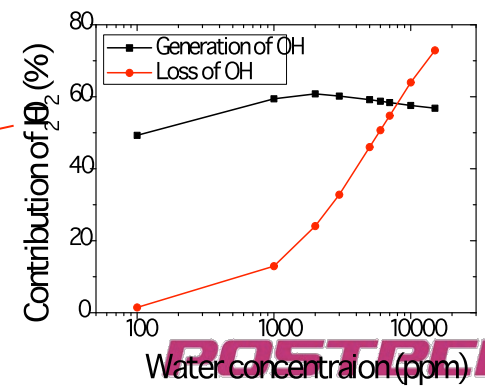

Indirect Treatment: Considering Half-life Time and Diffusion

At the end of the nozzle (x=0)

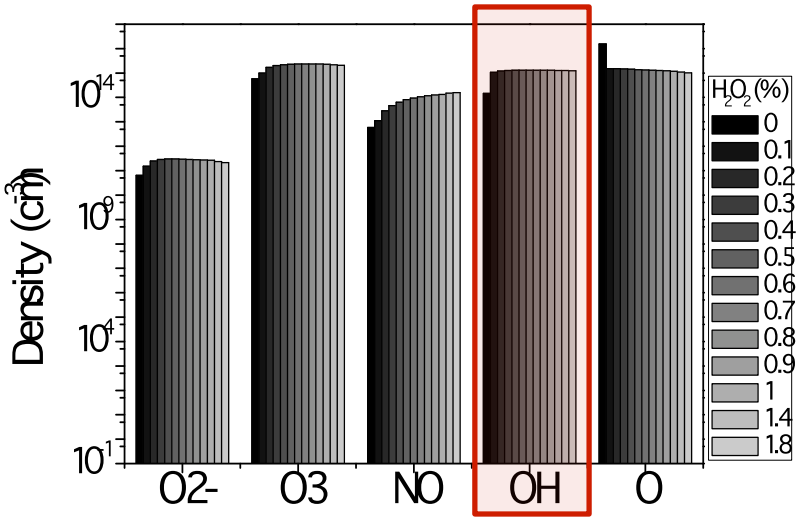

At the distance of 1 cm

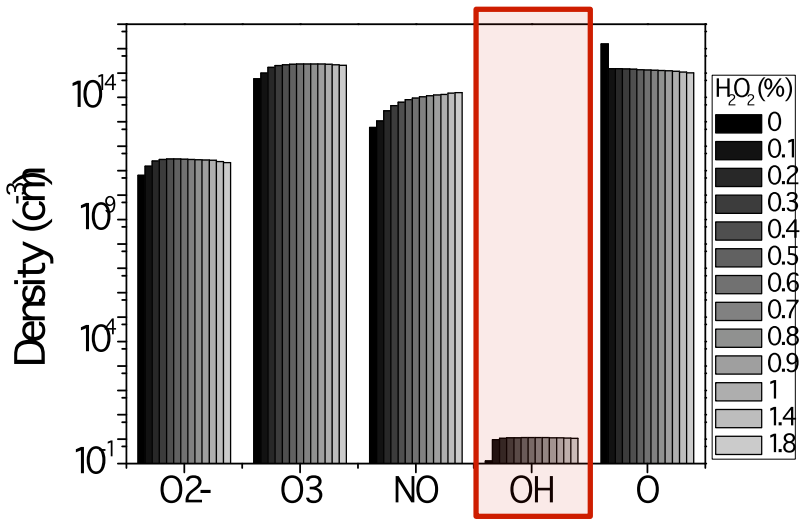

- In the indirect treatment case, O_3 and O_2^- might play a crucial role in the sterilization, because
  - 1. It is known that they have germicidal effects*[a] and are biologically toxic*[b].
    - *a. Laroussi M 2009, *IEEE Trans. Plasma Sci.* **37** 714-25
    - *b. Thannickal V J *et al.* 2000, *Am. J. Physiol. Lung Cell. Mol. Physiol.* **279**, L1005-28
  - 2. Their half-life distances (> 100m) are much larger than the usual distance (~cm) between the plasma nozzle and a treated sample, so their density is sufficient to show effects.
  - 3. They have maximum density point (O_2^-: 0.5 % and O_3: 0.7 % of H_2O_2) in common, which show good agreement with sterilization experiment results.

- On the other hand, OH density decreases rapidly as the distance increases because its half-life distance is too short (~0.02 cm). But it might still be crucial in direct plasma treatment case.

2. Departure from Paschen in Microgaps: PIC Results before Expt.

Onset of field emissions

Argon at 1 atm

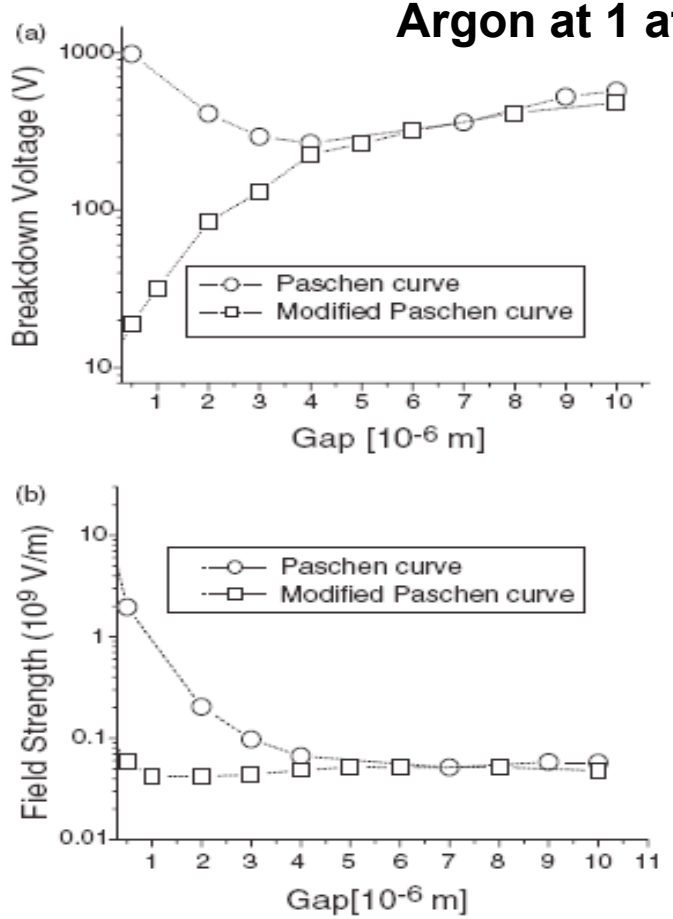

Figure 2. (*a*) Breakdown voltage and (*b*) electric field strength as a function of the gap size for argon at 1 atm. Results obtained by using energy and angular dependence of the yield per ion [27] (○) are compared with the results obtained when field-emissions are taken into account (□).

WILEY-VCH Verlag Berlin GmbH

498 **5th June 2007** *17 Atmospheric glow discharges*

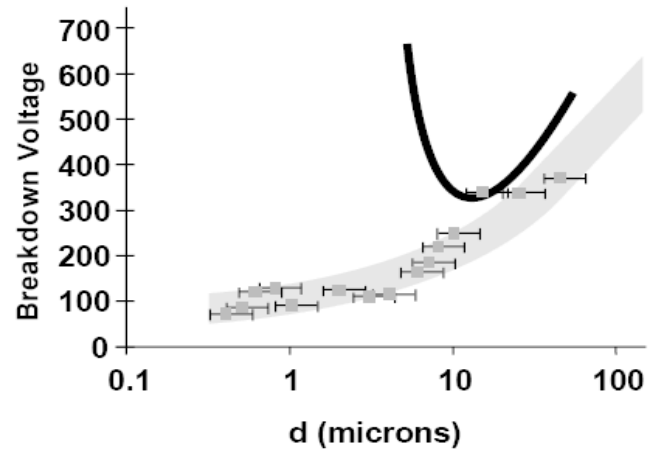

Figure 17.1: Paschen Curve for air (dark line) derived from low pressure pD scaling. Gray band shows experimental data [3, 4] taken for small gaps in air at atmospheric pressure.

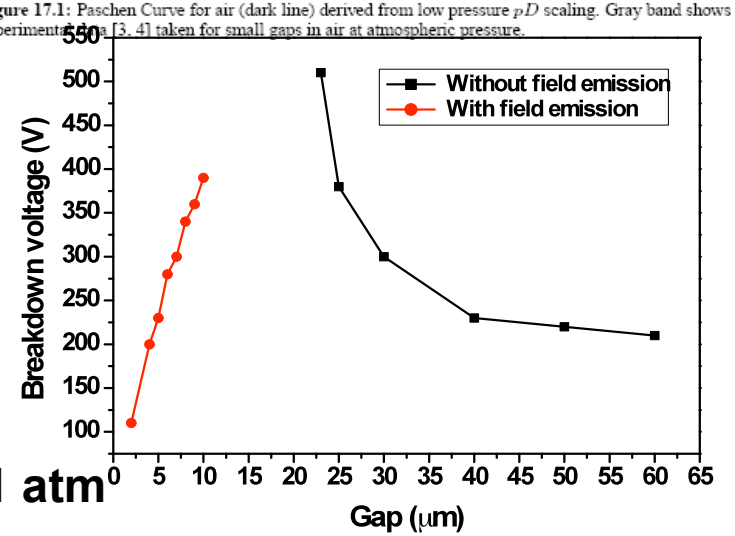

Helium at 1 atm

[Ref.] M. Radmilovic-Radjenovic, JK Lee, et al., J. Phys. D 38, 950 (2005)

Relation between N_D and N_C

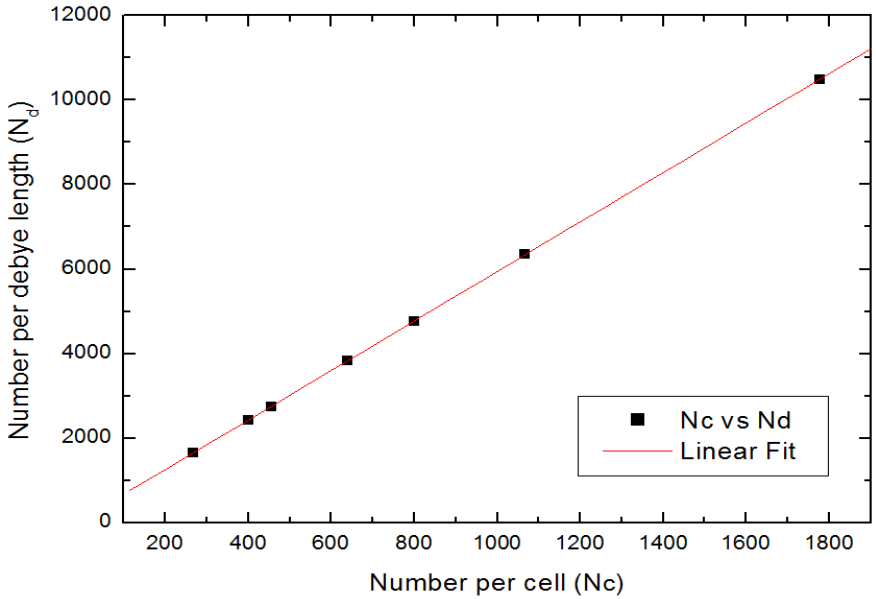

Slope of linear fitted line = 5.86

Nd / Nc = 5.86

Similar with difference between ΔX and λ_D (Debye length)

λ_D / ΔX = 6.007

$$N_D / N_C = 5.86 \approx \lambda_D / \Delta X = 6.007$$

- Relation between calculated **N_D and N_C** is similar with relation between calculated **λ_D and N_C** .

POSTECH

Electron density with variations of N_C and N_D

H. C. Kim's case

Ref: J.Phys. D : Appl. Phys. 38 (2005) R 283- R301

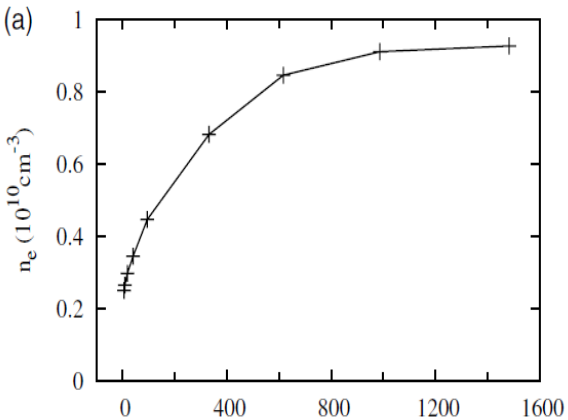

H. Y . Kim's case

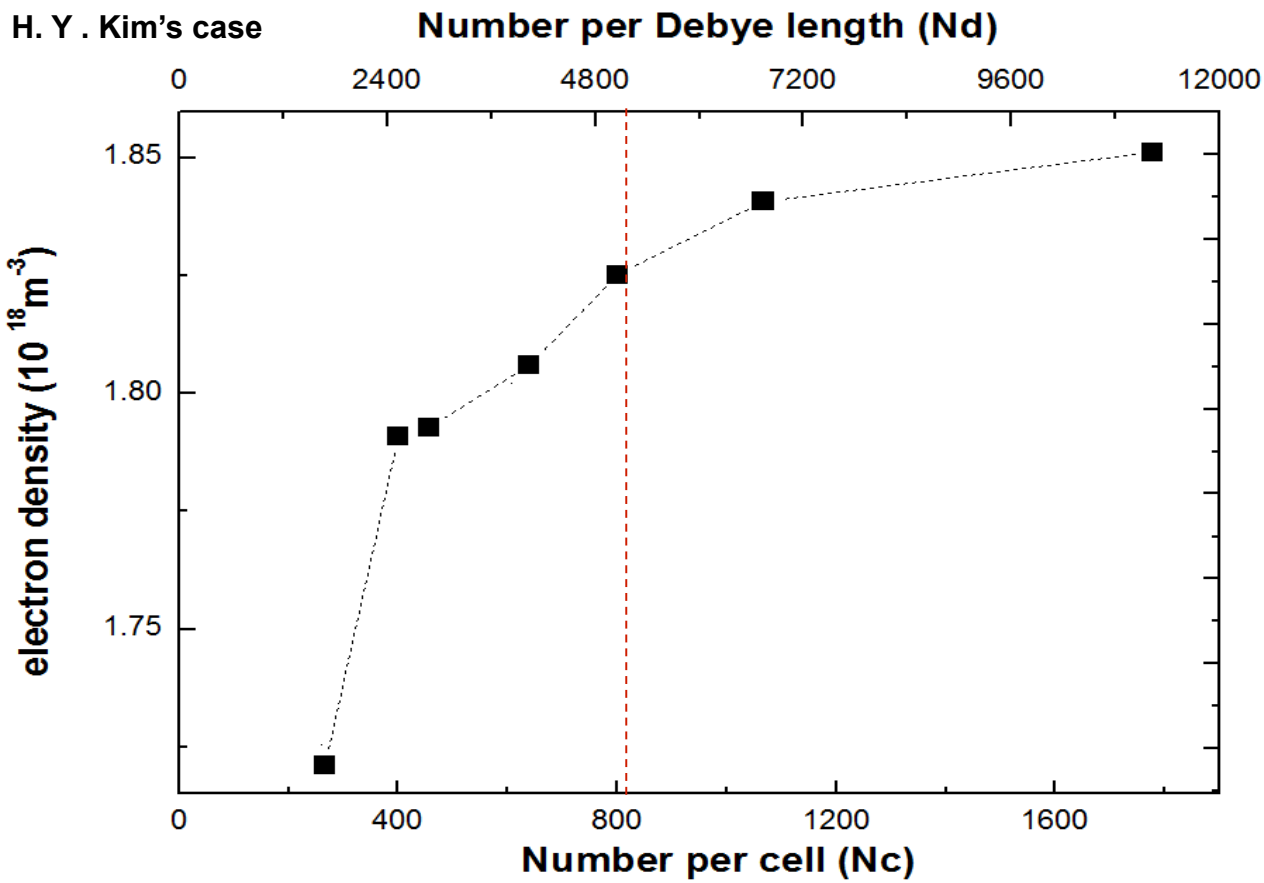

Our Simulation condition

- Gas pressure: **760 Torr**
- Gap size: **200 μm**
- Gas: **Ar**
- Frequency: **500MHz**
- Voltage : 130V
- Grid: **100**
- Area: **0.01 m²**

- Simulation result at the atmospheric pressure shows similar trend with low pressure case (H.C.Kim's case)
- Electron density is starting to saturate after 800 of N_C (≈ 4800 of N_D)

POSTECH